Three-dimensional visualization of the renal microcirculation using laser speckle contrast imaging

MSc thesis Mechanical Engineering

Lisanne van Ooijen

TU Delft

Erasmus MC

Three-dimensional visualization of the renal microcirculation using laser speckle contrast imaging

by

L.S. van Ooijen

to obtain the degree of Master of Science
at the Delft University of Technology,
to be defended publicly on December 2, 2022 at 10:00.

Student number:	4530853	
Project duration:	January, 2022 – November, 2022	
Thesis committee:	Prof. dr. J. Dankelman,	TU Delft, supervisor
	Dr. R. W. F. de Bruin, PhD	Erasmus MC, supervisor
	Y. Fang, MD	Erasmus MC, supervisor
	Dr. ir. F. J. H. Gijsen, PhD	TU Delft, committee member

This thesis is confidential and cannot be made public until December 2024.

TU Delft

Erasmus MC
Universitair Medisch Centrum Rotterdam

Abstract

In the Netherlands, over 12% of the population has chronic kidney damage resulting in about 2000 patients with renal failure each year. Replacement of the kidney function by transplantation is desired, but due to a shortage of donor kidneys, the waiting list for a transplant is long. Extending the criteria that donors must meet can reduce the waiting list, but it is necessary that these organs are still of sufficient quality. Initial studies indicate that using the normothermic machine perfusion (NMP) preservation method results in better transplant outcomes and possibly improves donor kidneys' quality. The quality of the organ during NMP can be used as a potential biomarker for graft survival. However, what is still missing is a reliable way to test the quality during NMP. Laser speckle contrast imaging (LSCI) is a non-invasive, continuous, real-time imaging technique that can visualize tissue perfusion. In this study, a method is designed to visualize the perfusion over the entire surface of normothermic machine-perfused kidneys using LSCI. A three-dimensional (3D) perfusion model is developed based on two-dimensional (2D) LSCI images. This method can then be used to determine the quality of the perfusion of donor kidneys before they are transplanted.

A method is designed to obtain LSCI data of porcine kidneys undergoing NMP. Data is recorded during the first 100 minutes of NMP to evaluate the relationship between renal arterial blood flow and perfusion. The kidneys are then placed in six different positions from which LSCI data is collected. The angle of incidence of the LSCI device changes over the convex surface of the kidney. Therefore, the influence of this angle on the measured perfusion is investigated by varying the angle of incidence between 0° and 40°. Using shape from silhouettes, a 3D model is made from each kidney. The 2D LSCI data is given depth using the 3D model by assigning each pixel a 3D coordinate. The perfusion model is validated by comparing the perfusion model for the situation where no ischemia is present in the kidney and the situation where ischemia is present in the kidney.

The designed method and setup made it possible to obtain perfusion data over the vast majority of the surface of the kidneys. Further, the results show a positive linear correlation between measured perfusion and arterial blood flow in each kidney. Measured perfusion did differ significantly for an angle of incidence of 40° compared to 0°; the decrease was 14%. A decrease of 27% was measured by dividing the perfusion by the flow to correct for the flow differences between the measurements. With the collected perfusion data, a 3D visualization was made. 3D models from all kidneys could be used for this. A model has been made to calculate the angle of incidence over the 3D model. The 3D visualization was represented as a point cloud and allows for easy and fast viewing of the perfusion over the entire surface. Perfusion data measured at angles of incidence >40° has been removed.

Validating the model with induced ischemia showed that the 3D visualization can indicate significant perfusion differences caused by ischemia. This makes LSCI a promising method for determining perfusion quality.

Preface

Before you lies my master thesis “Three-dimensional visualization of the renal microcirculation using laser speckle contrast imaging”. It has been written to fulfill the graduation requirements of the master’s degree in Mechanical Engineering, track BioMechanical Design, at the Delft University of Technology. I have been working on this thesis from January 2022 to November 2022. By handing in and defending this thesis, my study period will come to an end.

From the beginning of my study period, I have always been interested in using technical knowledge within the medical field. Therefore, I am very grateful for the opportunity to work on this thesis in collaboration with the Erasmus MC Transplant Institute. In this project, I was able to combine many different aspects of the medical and technical fields. As a result, I gained a lot of new knowledge in the medical field (about kidneys, microcirculation, and transplant processes), but I also learned a lot in the technical field (theory of laser speckle contrast imaging, principles of 3D imaging, and I improved my programming skills). I have had a very educational and pleasant period with the support of many people, and I want to thank some of them in particular.

I want to thank Ron de Bruin from the Erasmus MC for supervising me during the project. Our meetings were always very useful and motivating. Also, your detailed feedback was very helpful, and you were always available to answer my questions. Furthermore, I want to thank Dafsy Bouari for introducing me to normothermic machine perfusion and learning me all the practical stuff about the setup. Also, I want to thank Roy Fang for helping prepare the kidneys for the experiments.

Next, I want to thank Jenny Dankelman for her supervision during this project. Your support, guidance, and feedback were very helpful. Also, thank you for giving me the opportunity to work on this project in collaboration with the Erasmus MC.

Finally, I would like to thank my friends and family for their continuous support throughout my study. You always kept me motivated and believed in me that I could do it.

Enjoy reading my thesis!

L.S. van Ooijen
Delft, November 2022

Contents

List of Figures

List of Tables

Nomenclature

2D	two-dimensional
3D	three-dimensional
deg	degrees
FOV	field of view
HMP	hypothermic machine perfusion
LSCI	laser speckle contrast imaging
NMP	normothermic machine perfusion
PU	perfusion unit(s)
RGB	red, green, blue
ROI	region of interest

1 Introduction

1.1. Renal failure

In the Netherlands, over 12% of the population has chronic kidney damage resulting in about 2000 patients with renal failure each year [27, 28]. Renal failure occurs when the kidneys function for less than 15%. Kidneys play key roles in removing waste products and maintaining the water balance by filtering the blood. Therefore kidney function should be replaced in case of renal failure [24, 32]. Replacement of the functioning can be achieved by dialysis or a kidney transplant. Compared to patients with dialysis, patients with a kidney transplant have a longer life expectancy, so transplantation is desired. However, the waiting list for a kidney transplant is long due to the limited availability of donor kidneys.

1.2. Organ donation

The process of organ donation can be classified into three categories: living organ donation, donation after brain death, and donation after circulatory death. Donors must meet strict (age) requirements to donate an organ. This ensures that only the best organs are transplanted to keep survival rates high. The chances of survival are also dependent on the process of organ donation. In the period between removing the organ from the donor and placing the organ at the recipient, there is oxygen deficiency (ischemia) in the donor organ due to the absence of (oxygen-rich) blood supply. This ischemia can result in tissue injury and increases the longer the oxygen deficiency lasts. If there is too much damage, this can lead to graft failure. For living organ donation, the warm ischemia time (the period between stopping blood supply and initiation of cold organ preservation) is the shortest resulting in the highest graft survival rate, followed by donation after brain death and donation after circulatory death [21]. Rapid reperfusion is necessary to limit tissue damage. However, reperfusion itself can cause injury to the ischemic tissue too. This is called ischemia-reperfusion injury [1, 9, 30].

The number of transplants must be increased to reduce the waiting list for a donor kidney, but this also requires more donors. Extending the criteria that donors must meet can contribute to this. However, since the risk of poor-quality organs is higher in this group, it is necessary to determine the quality of the organs.

1.3. Organ preservation methods

Research has been going on for years into the most optimal process for a kidney transplantation to increase the organ's chances of survival. Static cold storage was the first method for preservation and has been the standard in the Netherlands for a long time. Immediately after removal, the kidney is flushed with a cold perfusion fluid. This removes blood and clots and cools the kidney quickly from the inside. The kidney is then placed in a bag of perfusion fluid and kept on ice in an organ box. By preserving the kidney under hypothermic conditions, metabolism is reduced, and injury from ischemia is limited. Due to its low costs and simplicity, the method has been widely used as the standard preservation method for years [6, 29, 36].

Hypothermic machine perfusion (HMP) is currently the standard in the Netherlands. Immediately after removal, the kidney is flushed with a cold perfusion fluid. The kidney is then connected to a pump that allows perfusion fluid at a temperature of 4 degrees Celsius to flow through the kidney for a longer period of time. The advantages of this method are that oxygen and medication can be added to the perfusion fluid, and the continuous flow can remove toxic metabolic waste products [6, 13, 36].

At this time, research is also being conducted into perfusing kidneys with warm perfusion fluid. This method, called normothermic machine perfusion (NMP), is similar to HMP except that the perfusate pumped through the kidney is at body temperature. Further, the perfusate consists of blood, perfusion fluid, and medication. The perfusate is oxygenated to simulate the body's environment. Initial studies show that these kidneys have better transplant outcomes. It is also being investigated whether the method can be used to improve the quality of the donor kidney, which has a lot of added value when using extended criteria donors [15, 17, 19, 37].

1.4. Problem definition

By applying NMP, the functioning of the kidney can be examined even before the kidney is transplanted to the recipient. Possible ischemia or non-functioning of the circulation can be detected in advance. However, at this moment, there is no reliable way of testing the quality of the perfusion of the donor kidney during machine perfusion. Currently, the quality of perfusion is assessed based on the color of the entire kidney, see Figure 1.1, but this only gives a general and subjective impression of the renal blood flow. An emerging technology called laser speckle contrast imaging (LSCI) can possibly be used for quality assessment of the perfusion of (extended criteria) donor kidneys to replace the current method. LSCI is a technique that can visualize the blood flow in more detail and can also detect microcirculation changes during machine perfusion.

Currently, experimentation is going on with the use of LSCI during NMP as a biomarker to predict graft outcome of the donor kidneys. Perfusion images of the ventral and dorsal sides of the kidney are taken and analyzed. However, a problem with LSCI is that the images are two-dimensional (2D), and the kidney is three-dimensional (3D). It is yet to be discovered whether and how this dimensional deviation affects the visualized perfusion of the kidney. In addition, the current setup of NMP allows only for perfusion images made of the ventral and dorsal sides of the kidney. As a result, it is not possible to estimate the perfusion quality across the entire kidney.

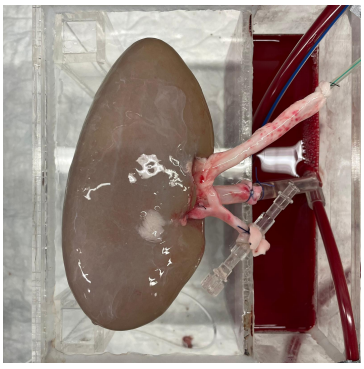

(a) No perfusion

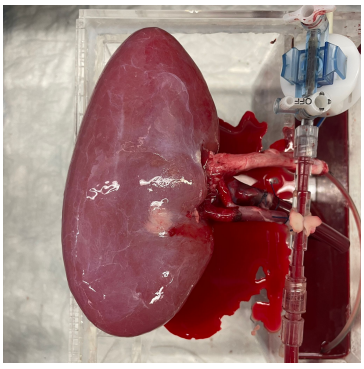

(b) Normal perfusion

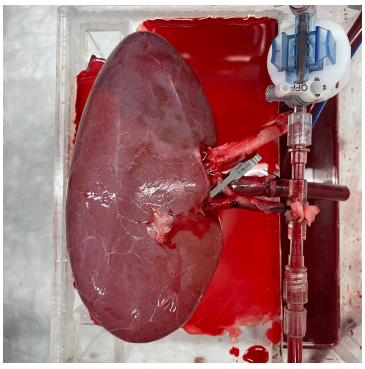

(c) Partial perfusion

Figure 1.1: Three situations of a kidney undergoing NMP resulting in different colors of the kidney's surface. In situation (a), the kidney is not perfused. Therefore no perfusion fluid is pumped through the renal circulation. The color of the kidney is brown, caused by the absence of perfusion fluid. In situation (b), the kidney is perfused normally. Therefore perfusion fluid is pumped through the renal circulation. The color of the kidney is red, caused by the red perfusion fluid. In situation (c), the kidney is perfused normally, but a branch of the renal artery is clamped. Therefore perfusion fluid is pumped through the lower part of the renal circulation only, causing ischemia in the upper part of the kidney. As a result, the color of the kidney at the upper part is different (darker) from the lower part (red).

1.5. Research objective

LSCI can possibly be used to replace the current perfusion quality assessment method by the color of the kidney. However, a method for this is still missing. Therefore the goal of this thesis is:

Design a method to visualize the perfusion over the entire surface of normothermic machine-perfused kidneys using laser speckle contrast imaging.

The study will be divided into smaller research objectives to achieve this goal.

Using laser speckle contrast imaging, two-dimensional perfusion recordings can be obtained. Research objectives belonging to this are defined as follows:

1. Design a setup and method to obtain two-dimensional perfusion recordings of the entire surface of the kidney.
2. Find out what the relationship is between the perfusion values measured with LSCI and the flow of the blood pumped through the kidney.
3. Find out how the convex surface of the kidney influences the perfusion values obtained with LSCI.

After obtaining the perfusion data using the laser speckle contrast imager, the data will be combined and processed into a visualization of the entire surface perfusion. Research objectives belonging to this are defined as follows:

4. Design a method to obtain a three-dimensional model of the kidney.
5. Combine the perfusion recordings and the three-dimensional model of the kidney into a three-dimensional perfusion model of the kidney.
6. Validate the perfusion model by comparing kidneys with and without ischemia.

1.6. Layout of this thesis

The structure of this thesis is defined as follows. In Chapter 2, LSCI is introduced, and experiments to obtain perfusion data of the kidney are performed. First, background information is given about the theory of LSCI and its application. Next, the method for performing LSCI measurements on kidneys is described, and its results are given and discussed. Smaller research objectives 1-3 are covered. Chapter 3 provides the method used to reach smaller research objectives 4-6. A three-dimensional model is made of each kidney, and the LSCI data is combined with the three-dimensional kidney model into the three-dimensional visualization of the perfusion. Lastly, the perfusion model is validated by comparing models with and without ischemia. At the end of the chapter, the perfusion model is discussed. The conclusion is given in Chapter 4.

2

Laser speckle contrast imaging experiments

The technique laser speckle contrast imaging is used to collect perfusion data of the renal microcirculation. This perfusion data is used for the 3D visualization. In this chapter, in Section 2.1, background information is given about the working principle of LSCI, the use of LSCI for blood flow assessment, and the application of LSCI in practice on a convex surface. Section 2.2 describes the method for performing LSCI experiments on porcine kidneys. The setup is described in detail, and the protocol for making perfusion recordings is explained. The protocol includes making recordings of the entire surface of the kidney (research objective 1), making recordings over time for the relationship between perfusion and blood flow (research objective 2), and making recordings with different angles of incidence of the camera (research objective 3). Recordings of the entire surface of the kidney are repeated when the blood flow is partly occluded to mimic ischemia (research objective 6). Section 2.2.3 describes the data processing and analysis method, and in Sections 2.3 and 2.4, the results are given and discussed. Results from this chapter are used in Chapter 3 for the 3D perfusion model.

2.1. Background

2.1.1. Working principle

LSCI is a real-time, continuous, and non-invasive imaging modality that can visualize the movement of particles. LSCI relies on the blurring effect of the speckle phenomenon. A speckle pattern is formed when a scattering object is illuminated by coherent light (a laser). This speckle pattern is the interference pattern formed by the backscattered light from the scattering object. A camera is used to observe the backscattered light. Due to slightly different positions and paths the backscattered light travels to reach the observer, the observer images diffraction with darker and brighter spots. The speckle pattern consists of static and dynamic speckles. Static speckles are formed by particles that do not move over time, and dynamic speckles are formed by particles that move over time [2, 4, 16, 34]. An example of a speckle image is given in Figure 2.1.

When Fercher and Briers first described the theory in 1981, only the difference between locations with and without flow was visible [11]. Over time the principle improved by using an exposure time longer than the least intense speckle. This shows a blurring pattern in the visualization, which is the result of moving particles. Areas with an increased flow are more blurred than areas with lower flow amounts. The rapid fluctuations of the speckles cause this [3, 10]. From the blurring effect, the speckle contrast K can be computed using the following equation:

$$K = \frac{\sigma}{\langle I \rangle} \tag{2.1}$$

where σ is the standard deviation of the intensity I, and $\langle I \rangle$ is the mean intensity. The speckle contrast can be calculated temporal (over time), spatial (in space), and spatio-temporal by combining both. The

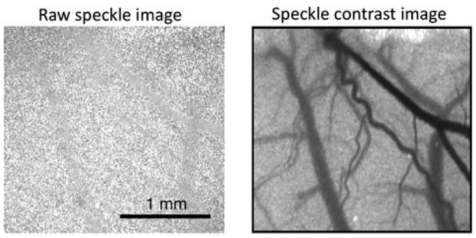

Figure 2.1: Raw speckle image (left) vs. speckle contrast image (right). Image retrieved from [31].

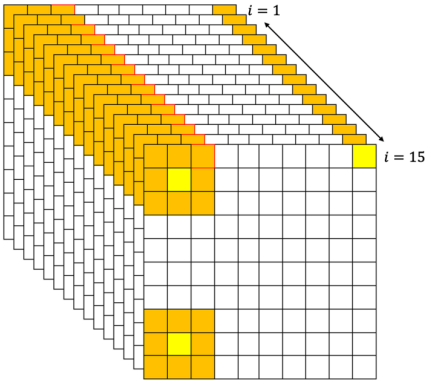

Figure 2.2: A matrix of pixels used to calculate the contrast spatial, temporal, and spatio-temporal. Image retrieved from [16].

temporal contrast is calculated using a single pixel over multiple frames and has a high spatial resolution (top right corner in Figure 2.2). Spatial contrast is calculated using multiple pixels over a single frame and has a high temporal resolution (bottom left corner in Figure 2.2). Spatio-temporal combines both methods and has both advantages (top left corner in Figure 2.2) [12, 16]. Spatial speckle contrast is optimally computed over windows (kernels) with 5x5 or 7x7 pixels [4].

A typical setup for LSCI consists of a laser, camera, object-to-image, and a computer with software to calculate the speckle contrast. Currently, computer software can give speckle contrast images in color, indicating the differences in movement of particles. Figure 2.3 shows a typical speckle contrast image in color. What is interesting is the difference in exposure times used. If the exposure time is too short, contrast differences are hard to notice, but with larger exposure times, blurring takes over.

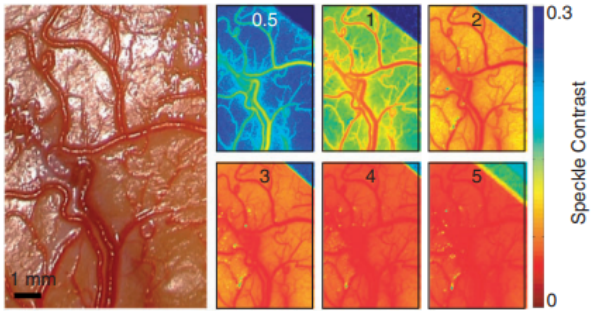

Figure 2.3: A colored photograph of blood vessels in the cortical area and corresponding speckle contrast images with exposure times ranging from 0.5 to 5 ms. A low speckle contrast *K* represents more blurring than a higher speckle contrast. When the exposure time is longer, blurring takes over. Image retrieved from [33].

LSCI can be used to visualize blood flow. Moving red blood cells form dynamic particles and blur the speckle image. Blood flow can be related to the speckle contrast because the Lorentzian velocity distribution, which is valid for Brownian motion, can be used to express the speckle contrast K related to the camera integration time T and the correlation time t_c [22]:

$$K = \frac{\sigma}{\langle I \rangle} = \left\{ \frac{\tau_c}{2T} \left[1 - e^{\left(\frac{-2T}{\tau_c} \right)} \right] \right\}^{\frac{1}{2}} \tag{2.2}$$

The speckle contrast values vary between 0 and 1, with 1 indicating no blurring since no motion is present and 0 indicating blurring of all speckles due to the fastest motion [10]. However, in practice, the speckle contrast measured is in the range of K = 0 to K = 0.5. This simplifies Equation 2.2 to:

$$K = \frac{\sigma}{\langle I \rangle} = \left(\frac{\tau_c}{2T} \right)^{\frac{1}{2}} \tag{2.3}$$

The speckle correlation time τ_c is inversely proportional to the speckle velocity ($\tau_c \propto \frac{1}{V}$). Therefore, by assuming that the perfusion is proportional to the speckle velocity, blood flow can be related to speckle contrast as follows:

$$\text{perfusion} \propto \left(\frac{\langle I \rangle}{\sigma}\right)^2 \tag{2.4}$$

The measurements performed with LSCI are not absolute values of blood flow nor linear related to absolute flow. Measured values are expressed in a relative unit called 'perfusion unit' (PU). A larger value of perfusion units corresponds to more perfusion, which means more movement of red blood cells. The perfusion unit is relative to a reference measurement obtained by calibration [2, 3, 4].

LSCI has a limitation on the depth it can reach because it is limited by scattering. Therefore LSCI can only be performed at the surface [7]. Davis et al. (2014) found that almost all scattering (95%) occurs in the top superficial 700 μm of tissue [8]. The actual depth that can be reached depends on the vascular structure in the superficial tissue. Larger diameter vessels have more possibility of multiple scattering within the vessels.

2.1.2. LSCI for quality assessment of kidneys

The function of kidneys is to filter the blood to remove waste products and maintain the body's water balance. The kidneys receive about 20% of cardiac output. Blood enters the kidneys through the renal arteries and leaves the kidneys through the renal veins. Waste products and water leave the kidney as urine through the ureter. In the kidney, the renal artery branches into narrowing arteries leading to the nephrons, where the blood is filtered. The filtering process starts in the renal cortex (the outer part of the kidney). Here ultrafiltration takes place in the glomeruli. The filtering continues deeper in the kidney in the renal medulla [24]. Since part of the renal microcirculation needed for filtering takes place in the superficial layer of tissue in the kidneys, LSCI can be applied during NMP. Perfusion observed with LSCI is part of the filtering process and contains useful information. When comparing the perfusion over time and between different locations, it is possible to see how it develops and in which areas the perfusion is absent or reduced. Reduced or absent perfusion represents ischemia and indicates the quality of the kidney.

2.1.3. LSCI on a convex surface

When applying LSCI to kidneys, it must be considered that the surface is not flat but convex. LSCI is a 2D imaging modality initially created to image 2D surfaces. When applying LSCI to a convex surface, there are two important variables to consider in the setup. The distance between the LSCI device and the kidney and the angle of incidence of the LSCI device on the kidney.

The distance between the LSCI device and the kidney differs per location on the surface of the kidney. The distance is smallest at the center of the surface where the LSCI device is positioned perpendicularly above the kidney and increases towards the edge of the kidney. In the experiments of this study, the distance should be set to ensure the entire kidney contour lies in the field of view (FOV) of the camera. The distance will, therefore, not be similar for each location during a recording. The kidney will also be placed in different positions, resulting in different distances between recordings. For the experiments in this thesis, the LSCI device moorO_2Flo (Moor Instruments Ltd) is used. The moorO_2Flo has a working distance ranging from 100-380 mm. Studies by Mahé et al. (2011) and Zötterman et al. (2017) have researched the influence of distance on the perfusion value. Outcomes show no significant difference in the measured perfusion between distances ranging from 15 to 40 cm and 10 to 30 cm [23, 39]. Therefore, it is assumed that the various distances in the experiments do not influence the measured perfusion values. The distance between the kidney and the moorO_2Flo will be set such that the entire contour lies in the FOV and the distance is within the working range of the device.

The laser's angle of incidence on the object's surface is also important for convex surfaces. The angle of incidence, expressed in degrees (deg), is the angle between the incident laser beam on the object and the line perpendicular to the surface at the point of incidence. For the convex kidney, the angle of incidence differs per location on the surface. In the middle of the kidney, the angle will be perpendicular

(0°), but towards the edges of the contour, the angle of incidence will increase to, at most, 90°. Results of studies by Lindahl et al. (2013), Stoianovici et al. (2011), and Zötterman et al. (2017) indicate that the angle of incidence does not affect the measured perfusion for angles less than 45° [20, 35, 39]. However, the results of the study of Molnár et al. (2017) do indicate an effect on the measured perfusion for an angle of only 10° [25]. The review by Vaz et al. (2016) considers the effect of the Brewster's angle and that the perfusion value may be higher at some angle above 0° but concludes that it has not been explored in the field yet and more studies should be performed to gain insight into the optimal angle [38]. Due to the diverse study outcomes and limited knowledge about the angle of incidence, in this study, additional research will be conducted into the influence of the angle of incidence on the measured perfusion.

2.2. Method

Three different experiments are performed with LSCI on porcine kidneys. First, an experiment to determine the relationship between flow and perfusion, then, an experiment to determine the influence of the angle of incidence, and lastly, an experiment to collect perfusion data over the entire surface of the kidney. This section will describe the setup, the protocol, and how the data is processed and analyzed.

2.2.1. Setup

Normothermic machine perfusion

The experiments are performed on *ex vivo* normothermic machine-perfused porcine kidneys. Once a week, porcine kidneys are collected at a local slaughterhouse. After receiving them, the kidneys are separated and flushed with a cold perfusion fluid (Ringerslactate) to remove blood and clots. Then the kidneys are connected to HMP. The LifePort Kidney Transporter (Organ Recovery Systems) is used for this.

After returning from the slaughterhouse, the kidneys are connected to the NMP setup. The setup is built in one of the research labs of the Erasmus MC. NMP has the purpose of mimicking the climate of the kidney as it is in the body. Therefore warm, oxygen-rich perfusate is pumped through the kidney. The perfusate consists of blood, perfusion fluid, and medication. The working principle is described below. Figure 2.4 shows a schematic overview of the NMP setup, and Figure 2.5 shows the complete setup.

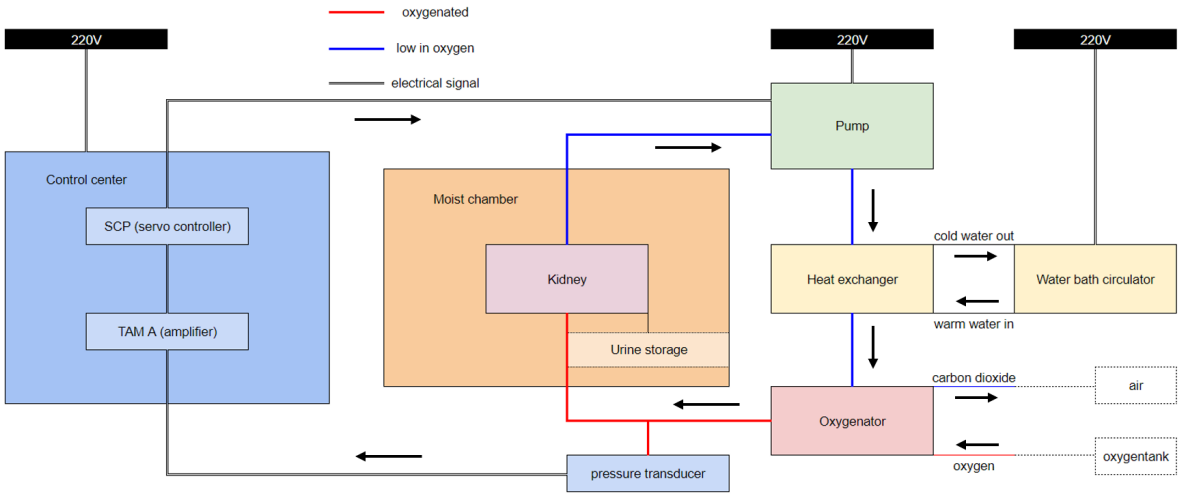

Figure 2.4: Schematic overview of the NMP setup.

Circulation starts at the bottom of the moist chamber (1), where the oxygen-poor perfusate is stored. A magnetic pump head connected to the gear pump (2) will let the perfusate flow from the bottom of the moist chamber through the pump head to the combined heat exchanger and oxygenator (3). Here the venous perfusate is oxygenated and heated. Perfusate then flows past the flow sensor (4) to check blood flow into the kidney. Then perfusate enters the renal artery by a cannula. Finally, venous perfusate leaves the kidney by the renal vein and drops into the reservoir of the moist chamber. A

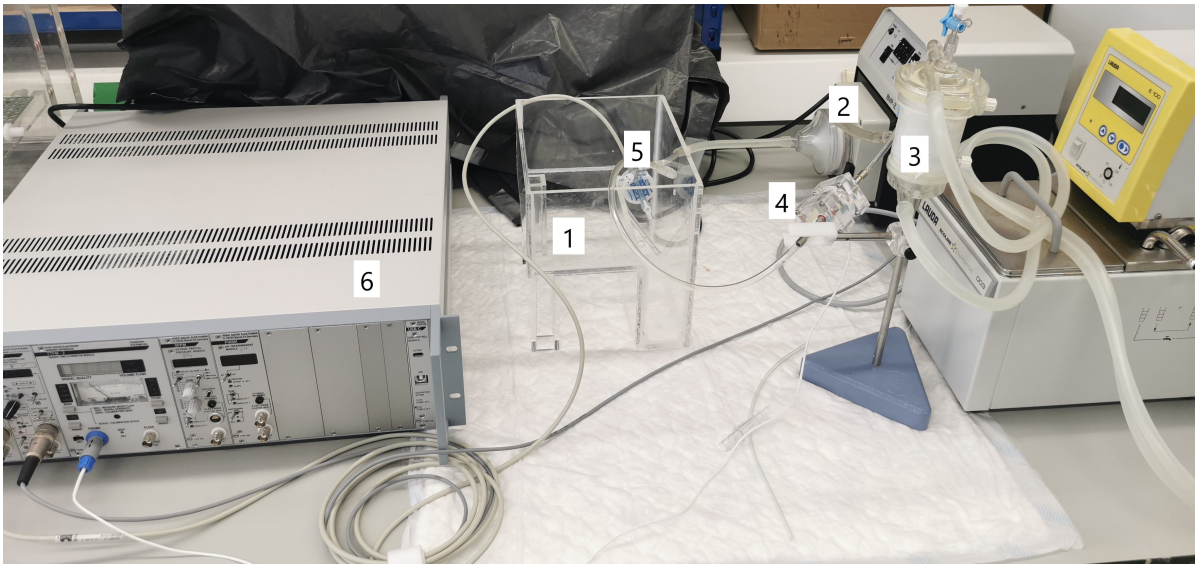

Figure 2.5: NMP setup in the Erasmus MC.

pressure sensor is connected to the cannula close to the renal artery to measure arterial pressure (5). The pressure and flow sensor data are sent to the control center (6). By comparing this feedback with the reference pressure, the control center will decide to adjust the gear pump speed to increase or decrease the flow and pressure.

1. Moist chamber
The moist chamber is the chamber where the kidney is placed inside. The chamber is heated and humidified to mimic the kidney's natural environment. The renal artery is cannulated and connected in series with the flow circuit of the perfusate. Urine that is produced can be collected by cannulating the ureter. The moist chamber is newly designed for the LSCI experiments. It has a volume sufficient for 1 liter of perfusate. The kidney is positioned on a higher plateau. Perfusate leaving the renal vein flows back into the reservoir. Therefore the edge of the reservoir could be made of minimal height, leaving sufficient space to reposition the kidney in all desired positions, as described later in this section. The moist chamber in Figure 2.5 is a version initially designed for making LSCI recordings without repositioning the kidney. Figure 2.8 shows the moist chamber used in the experiments of this thesis. The reservoir is made of laser-cut transparent PMMA with a thickness of 5 mm. Parts are glued with PMMA glue (Acrifix) and sealed with silicone sealant (Ottoseal S72).

2. Pump
A gear pump (BVP-Z gear pump, ISMATEC) is used for pumping the perfusate around. The first step is pumping the perfusate from the moist chamber through the pump head to the combined oxygenator and heat exchanger. The system uses constant pressure, and the control center controls the pump to achieve this constant pressure of approximately 70 mmHg.

3. Oxygenator & heat exchanger
Oxygen will be used during filtering as the perfusate flows through the kidney. Perfusate leaving the kidney, therefore, contains less oxygen. The oxygenator supplements the oxygen level in the perfusate. The setup is connected to an oxygen bottle that sends 500 mL of oxygen per minute through the oxygenator. The heat exchanger ensures that the perfusate is heated to the body temperature of 37 degrees Celsius. A heat bath (Lauda Ecoline Staredition E100) is connected to the combined heat exchanger/oxygenator. Warm water will run through the heat exchanger from bottom to top.

4. Flow sensor
A flow sensor measures the amount of perfusate that flows into the kidney per minute, the arterial blood flow (mL/min). It is connected to the control center where the output is given. The sensor is not involved

in the automatic control system since the system is pressure regulated.

5. Pressure sensor
In the tubing, directly before the renal artery, a branch to the pressure transducer (APT300, Harvard Apparatus), which measures the arterial pressure in the system, is present. The mechanical pressure is converted into an electrical signal and sent to the control center. In the control center, it is compared with the reference value. If necessary, the pump is controlled to run faster or slower. Before using the pressure transducer, it must be calibrated by zeroing the pressure to ambient pressure.

6. Control center
The control center is not in series with the perfusate circuit since no perfusate is involved in the tubing. Instead, the control center receives the electrical signal from the pressure transducer, the pressure of the arterial flow. The signal is sent via an amplifier (TAM-A, HSE) to the servo controller module, where the pressure is controlled. The servo controller module works as a PID controller and compares the received signal with the reference value. If the received signal is too low (low blood pressure), the pump is commanded to run faster; if the received signal is too high (high blood pressure), the pump is commanded to run more slowly.

LSCI device
The LSCI device moorO_2Flo is used to perform the kidney's microcirculation perfusion recordings. The moorO_2Flo is a perfusion and oxygenation imager. It can image tissue perfusion and relative tissue oxyhemoglobin and deoxyhemoglobin concentration change. In this thesis, the device is only used to image tissue perfusion. Perfusion is measured in the relative quantity perfusion unit (PU). The working distance ranges from 100-380 mm, and the imaging area can be between 5.6 mm x 7.5 mm (maximum zoom, minimum distance) and 150 mm x 200 mm (minimum zoom, maximum distance). Two low-power visible aiming lasers (650 nm, collimated emission pattern) can be used to measure the distance. The two lasers appear as a single point at a distance of 25 cm. The image resolution can be 116 by 150 pixels (low resolution) or 576 by 748 pixels (high resolution). Color photo/video images have a resolution of 580 by 752 pixels. Low-resolution recordings of 30 seconds are made with a frame rate of 20 Hz resulting in 601 frames for each recording. The measure mode is spatial with a kernel size of 5 by 5 pixels. The measurement laser emits a diverging circular beam with a wavelength of 764 nm $\pm$ 10 nm [22].

The device is placed perpendicular above the kidney. The contour of the kidney should always be in the FOV. Therefore the distance is set based on the size of the kidney but at a maximum distance of 380 mm above the kidney. In order to perform LSCI, the environment must be completely dark. A black cloth is used to achieve this by placing it over the setup. Further, the lights in the room are turned off. Vibrations in the environment must be limited. The LSCI device is started by connecting the device to power and running the program moorO_2Flo Measurement (Moor Instruments Ltd) on the Erasmus MC laptop designated for the LSCI measurements, which is connected to the LSCI device.

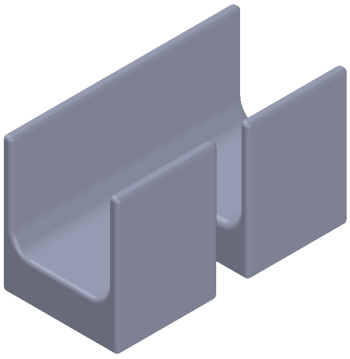

Figure 2.6: 3D-printed model used for placing the kidney in positions 3 and 4.

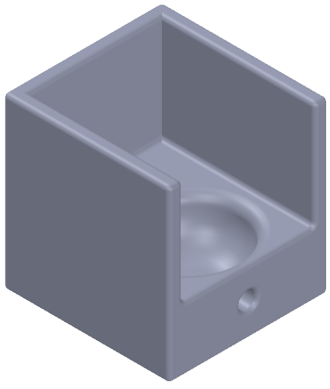

Figure 2.7: 3D-printed model used for placing the kidney in positions 5 and 6.

Kidney positions
During the experiments, the kidney is placed in different positions. Six positions are used to visualize all sides of the kidney. The primary and also starting position is position 1. In position 1, the renal hilum lies in the direction of the part of the reservoir containing the perfusate. The ureter is positioned to the right when viewed from the perfusate reservoir side. Later, the kidney is also placed in other positions. In position 2, the kidney is reversed from position 1, and the ureter is positioned to the left. In position 3, the renal hilum points upwards, and in position 4 downwards. To place the kidney in positions 3 and 4, a 3D-printed model that holds the kidney in place is used (Figure 2.6). In the model, an excision is made for the artery, vein, and ureter. In positions 5 and 6, the renal hilum again faces the perfusate reservoir side. In position 5, the ureter is directed downwards, and in position 6 upwards. For positions 5 and 6, again, a 3D-printed model is used to keep the kidney in place (Figure 2.7). An opening is made at the bottom of the 3D model to allow the perfusate to drain. Figure 2.8 gives a schematic overview of the kidney in six different positions in the reservoir.

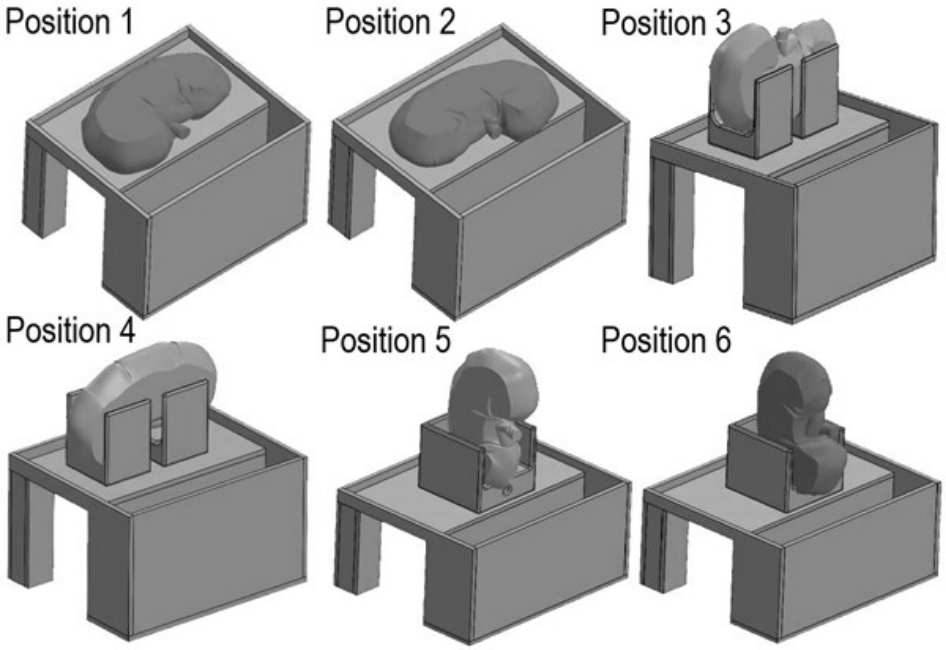

Figure 2.8: The kidney placed in the reservoir in six different positions. For positions 3 & 4 and positions 5 & 6, the 3D-printed models are used to keep the kidney in position.

2.2.2. Protocol
The LSCI experiments start when the kidney is connected to NMP. Connecting to NMP is time point zero (t = 0 min). The kidney is in position 1. In this subsection, the protocol is explained globally. The stepwise protocol for LSCI used during the experiments is attached in Appendix A.

Perfusion over time
Research objective 2 is to determine the relationship between the perfusion values measured with LSCI and the flow of blood pumped through the kidney. For this objective, perfusion recordings are made during the first 100 minutes of NMP. In this period, flow is still rising. After the kidney is connected to NMP, an LSCI recording is made every 10 minutes. The kidney remains in position 1 during this experiment. The recordings serve to show the progress of the perfusion in the kidney. For each recording, the arterial renal blood flow (mL/min) is measured with the flow sensor of the NMP setup.

Perfusion in different positions
For both the primary research objective and research objective 1, a method is needed to obtain 2D perfusion recordings of the entire surface of the kidney. Recordings are taken with the kidney placed in six different positions. The recordings take place after 100 minutes of NMP (t = 100 min) and are

taken in a time span of 10 minutes. Recordings are taken in ascending order starting with position 1 and ending with position 6. For each recording, the arterial flow is measured. For each measurement, it is essential that the contour of the kidney is entirely in the FOV and that the contour is straight in the plane, not at an angle. Moving the kidney to other positions is done by hand.
After the first set of recordings of the six positions, the experiment using different angles of incidence (as described below) is performed. After the angle of incidence experiment, the inferior branch of the artery is clamped with an artery clamp (Figure 2.10), and recordings of the six positions are repeated. By partly occluding the kidney, perfusion differences in the microcirculation arise from ischemia. Perfusion before and after clamping is compared. These recordings are used for research objective 6 to validate the 3D perfusion model.

Perfusion for different angles of incidence
Between taking the LSCI recordings with the kidney in different positions before and after clamping the inferior branch of the artery, LSCI recordings are taken for research objective 3. The angle of incidence of the moorO_2Flo is brought to different angles using a protractor. The kidney is placed in position 1 and remains in this position during the measurements. The first recording is with the LSCI device placed perpendicular above the kidney (0°). The upcoming recordings are with angles of incidence of 10°, 20°, 30°, and 40° (see Figure 2.9). During each measurement, the arterial flow is measured. The data collected from the recordings are used to analyze the influence of the convex shape on the perfusion outcomes.

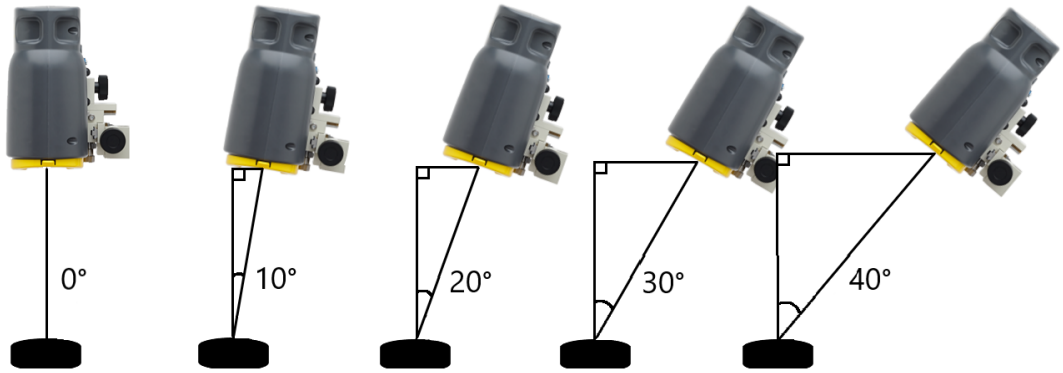

Figure 2.9: LSCI device with different angles of incidence on the kidney's surface.

2.2.3. Data processing and analysis

After performing the LSCI experiments on the porcine kidneys, the data is processed and analyzed. Data recorded with the moorO_2Flo and corresponding measurement software is opened and reviewed in the program moorO_2Flo Analysis (Moor Instruments Ltd). Perfusion data can be analyzed frame by frame, and regions of interest (ROIs) can be assigned. Colored images of the kidneys can also be viewed. MATLAB (MathWorks, Inc.) is used for data processing and analysis. Therefore perfusion data is exported to .mat files. Each recording consists of 601 frames, and each frame is a 116 by 150 pixels array. Pixel data is averaged over the 601 frames resulting in a mean perfusion array. Data processing and analysis depend on the research objectives. Different processing and analysis methods are described below.

Perfusion over time
Perfusion recordings of the different time points are compared per kidney. Perfusion images of the mean perfusion are used and plotted using the 'jet' colormap consisting of 256 colors with a range of 0 to 1000 PU, similar to the colormap used by the moorO_2Flo and corresponding measurement software. Three square ROIs are selected on the first frame, and mean perfusion is calculated and compared over time. Figure 2.11 shows the three ROIs. Linear correlation between the perfusion and flow is analyzed using Pearson's correlation coefficient r with a 95% confidence interval. The statistical analysis is performed using IBM SPSS Statistics for Windows, Version 26.0 (IBM Company, Armonk, NY).

Perfusion in different positions
Perfusion images of the different positions are compared per kidney. Perfusion images of the mean perfusion are used and plotted using the 'jet' colormap consisting of 256 colors with a range of 0 to 1000 PU. Histograms are made to analyze the perfusion distribution per position per kidney (before clamping). The ROIs, consisting of the exposed area of the kidney in each position, are selected manually in the MATLAB app image labeler. Then, the mean perfusion and standard deviation per position are calculated.

Perfusion for different angles of incidence
Perfusion is compared for five different angles of incidence. An ROI is selected manually in frame 1 of the recording and consists of a part of the surface with an angle of incidence of 0°. The ROI is copied for every recording with a changed angle of incidence and is adjusted manually to contain the same surface area as in the recording with an angle of incidence of 0°. Figures 2.12 and 2.13 show the ROI for the angle of incidence of 0° and the ROI for the angle of incidence of 40° on one of the kidneys.

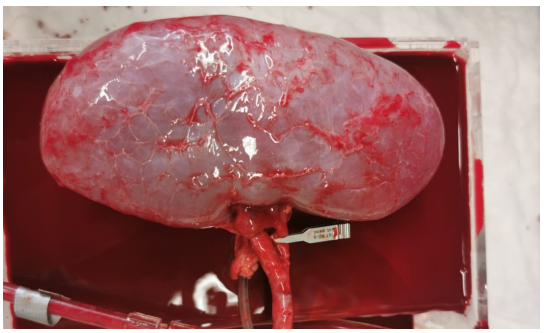

Figure 2.10: Inferior branch of the artery clamped with an artery clamp.

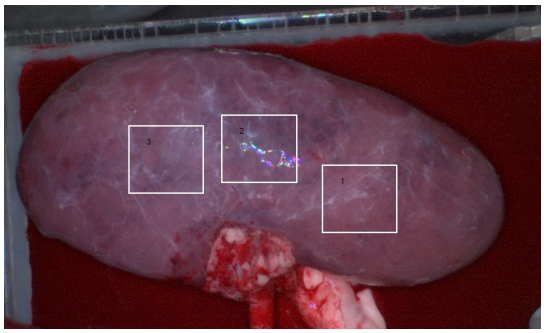

Figure 2.11: Three ROIs for recordings of first 100 minutes of NMP.

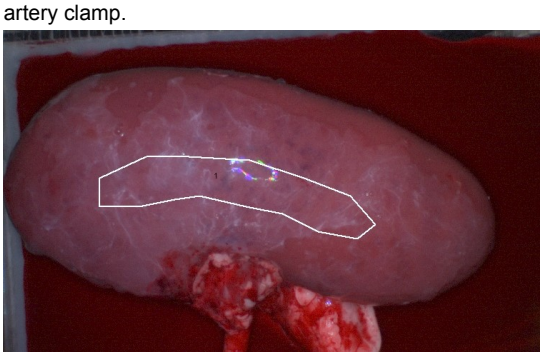

Figure 2.12: ROI for angle of incidence of 0°.

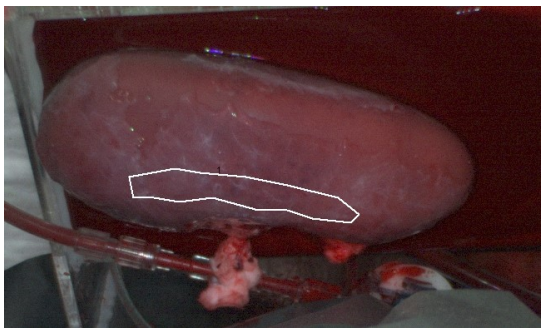

Figure 2.13: ROI for angle of incidence of 40°.

2.3. Results
In total, four porcine kidneys are connected to NMP and used to perform the LSCI experiments. The experiments were performed in two consecutive weeks. In both weeks, kidneys were collected from the slaughterhouse on Monday, and experiments were performed on Monday and Tuesday. The kidneys are numbered in ascending order based on the date of the experiment. For example, the first kidney is numbered 1, and the upcoming kidneys are 2, 3, and 4.

2.3.1. Perfusion in different positions
It was possible to make perfusion recordings from all four kidneys in all six positions. However, results differ per position and kidney. Perfusion images with the kidneys placed in the six positions are shown in Figure 2.14. For each kidney, images are shown before and after clamping the inferior branch of the artery. The inferior artery branch is the right branch in positions 1, 3, and 4, and the left branch in position 2. The images before clamping are on the top rows, and those after clamping are on the bottom. Corresponding data of the arterial flow is given in Table 2.1. Histograms with the perfusion distribution before clamping for each kidney per position are given in Appendix B. Appendix C shows colored photos of a kidney placed in the six positions both before and after clamping.

Positions 1 and 2
It is noticeable that the kidneys differ in size. For kidneys 1, 2, and 4, the length of the kidney was within the FOV of the camera. However, the length of kidney 3 did not entirely fit the FOV. Meanwhile, the width always fitted the FOV. Positioning the kidney in positions 1 and 2 did not cause any problems, and the flow stayed the same. Looking at the perfusion values, it is noticeable that the perfusion decreases towards the edge of the kidneys.

Positions 3 and 4
The length of the kidney is also essential for positions 3 and 4. Kidney 3 did not fit in the FOV. Position 3 represents the side of the renal hilum. The artery, vein, and ureter partially blocked the view of the surface of the kidney. In position 4, this is not the case. The kidneys all fitted in the 3D-printed model used to position them. When the kidney was repositioned, the flow in the kidney decreased in some cases (kidney 1 before clamping, kidney 3 after clamping, and kidney 4 both before and after clamping). Also, in positions 3 and 4, the perfusion decreases towards the outer edge.

Positions 5 and 6
All kidneys fitted in the FOV in positions 5 and 6. However, positioning the kidneys using the 3D-printed model was difficult. A good balance had to be found to keep the kidney in the upright position. In the case of kidney 2, this was done by placing the kidney at an angle in the 3D-printed model. To get the contour straight into the FOV, the 3D-printed model is twisted a few degrees. The flow remained about equal to the flow in positions 3 and 4, except for kidney 3 in position 5 before clamping, where the flow decreased significantly to 60 mL/min.

Further, it is noticeable that the perfusion decreases towards the outer edge of the kidney. This is more visible on the side where the kidney does not lean against the 3D-printed model (top right in the figure in most cases). There is also an arc having a deviated perfusion running through the perfusion images. This is most visible in kidneys 3 and 4. Lastly, it is noticeable that the perfusion in positions 5 and 6 has higher overall values compared to positions 1 to 4.

Arterial flow (mL/min)	Position 1	Position 2	Position 3	Position 4	Position 5	Position 6
Kidney 1 before clamping	170	170	147	154	147	147
Kidney 1 after clamping	88	92	87	90	81	86
Kidney 2 before clamping	115	113	115	118	115	111
Kidney 2 after clamping	86	86	84	83	84	80
Kidney 3 before clamping	109	110	105	99	60	97
Kidney 3 after clamping	62	61	56	56	52	45
Kidney 4 before clamping	276	279	242	263	236	236
Kidney 4 after clamping	232	228	200	216	203	190

Table 2.1: Arterial flow (mL/min) during each measurement of four kidneys in six positions both before and after clamping.

All positions
Looking at the overall results, it is noticeable that perfusion images have unexpected dark blue spots, mainly at the same position. The size differs per position and kidney. Comparing the perfusion before and after clamping the inferior branch, it is easy to see that the perfusion has decreased in part of the kidney. The size of the part of the kidney with lower perfusion differs per kidney. In kidneys 1, 2,

and 3, the clamping is clearly visible in both position 1 and position 2. In kidney 4, however, there is no difference in position 2 after clamping compared to position 2 before clamping. Also, in kidney 4 in positions 3 and 6, large parts with perfusion can still be seen, whereas, in the other kidneys, the perfusion seems absent. Further, in kidneys 2 and 3, the overall perfusion is lower than in kidneys 1 and 4. In kidney 2, the perfusion in position 1 is lowest but increases over the positions.
Arterial flow differs significantly per kidney. Kidney 4 has the highest overall arterial flow, with a flow of 276 mL/min in position 1 before clamping. In kidney 3, the flow is much lower, with a flow of 109 mL/min in position 1 before clamping. Perfusion before clamping is higher than perfusion after clamping.
Lastly, it is noticeable that the background also takes a perfusion value. However, the kidney contour can clearly be differentiated from the background.

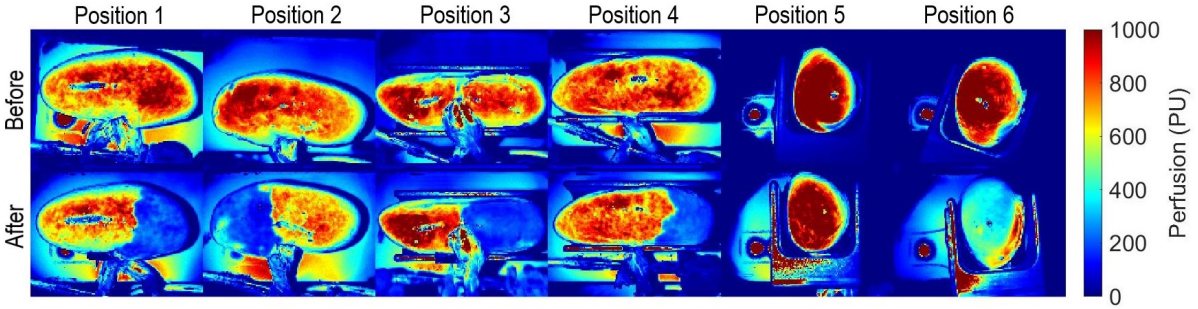

(a) Kidney 1

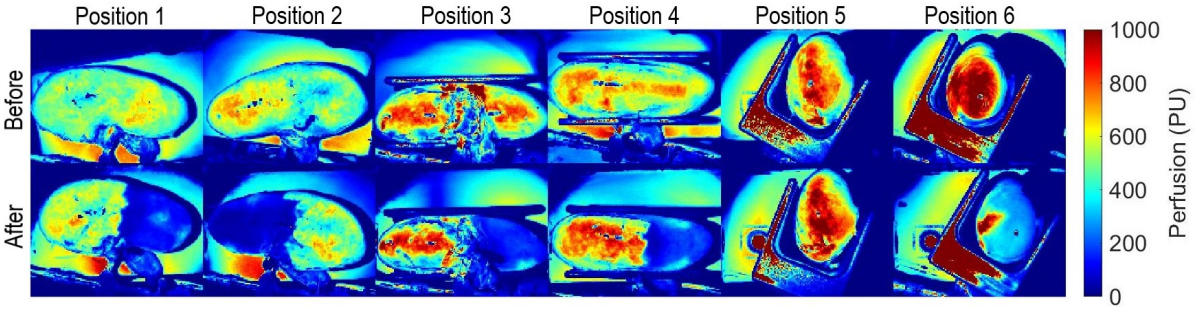

(b) Kidney 2

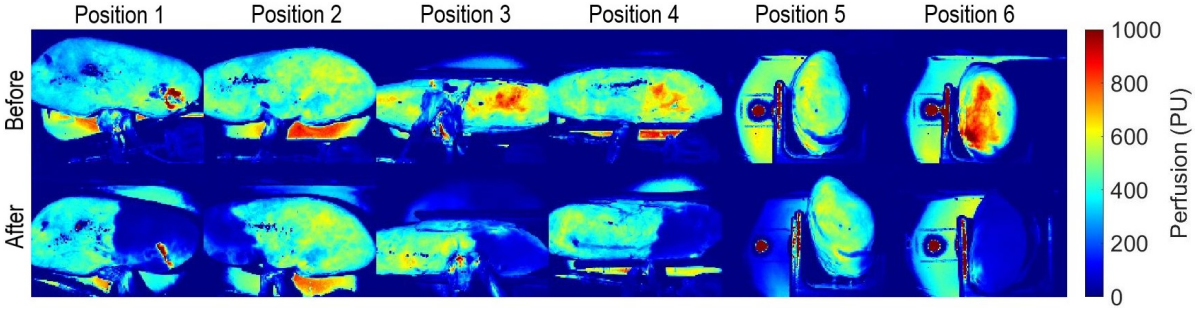

(c) Kidney 3

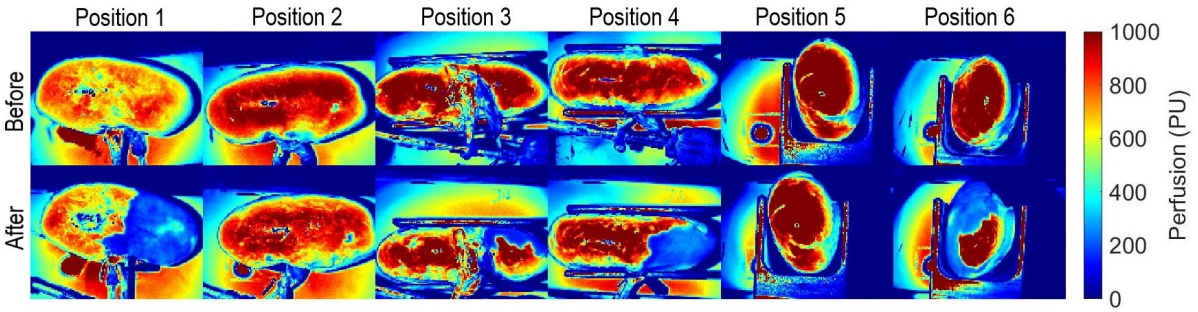

(d) Kidney 4

Figure 2.14: Perfusion of four kidneys in six positions both before and after clamping the inferior branch of the artery.

2.3.2. Perfusion and flow over time

Colored perfusion images of position 1 during the first 100 minutes of NMP are given in Figure 2.18. The images from the first 50 minutes are shown in the top row. The images from minutes 60 to 100 are shown in the bottom row. Figure 2.15 shows the flow's progress over time, and Figure 2.16 shows the progress of the perfusion over time.

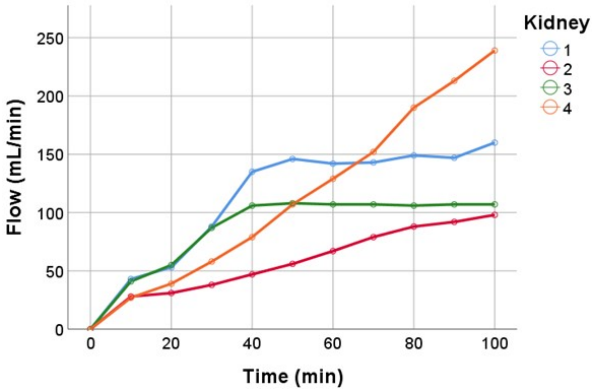

Figure 2.15: Arterial blood flow over time for the first 100 minutes of NMP.

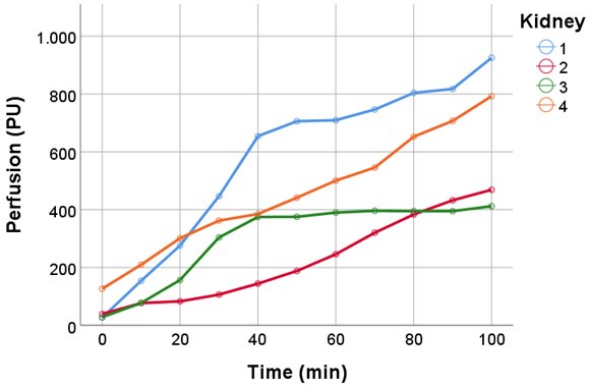

Figure 2.16: Perfusion over time for the first 100 minutes of NMP.

The linear correlation between perfusion and flow was measured using the Pearson correlation coefficient *r*. Figure 2.17 shows a scatterplot with the perfusion against the flow of the four kidneys. Pearson's correlation coefficient *r* was calculated for each kidney to assess the relationship between the perfusion and the flow. There was a strong positive correlation for each kidney between the variables ($r_1 = 0.984$, $r_2 = 0.991$, $r_3 = 0.995$, $r_4 = 0.994$). The relationship between the variables is in the 95% confidence interval since the calculated *r* values are higher than the table *r* value ($r = 0.632$ for 10 data points). The combined correlation coefficient for all kidneys ($r_{total} = 0.895$) indicates a positive correlation between the perfusion and the flow since the calculated *r* value is more than the table *r* value ($r = 0.312$ for 40 data points). The linear correlation is clearly visible in the graphs.

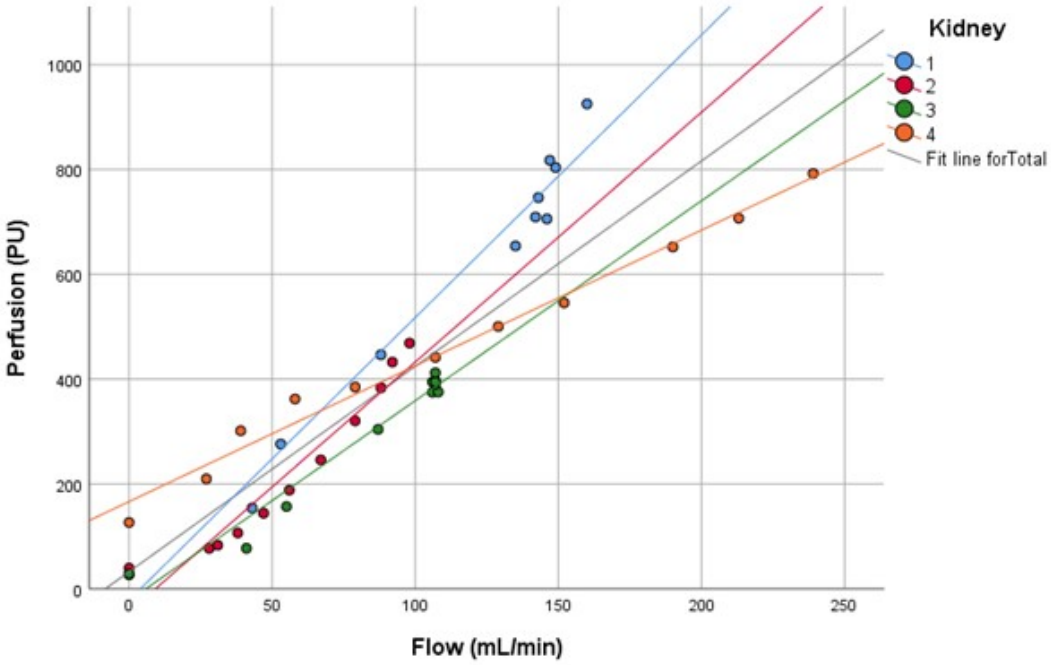

Figure 2.17: Correlation between the mean perfusion per ROI and the arterial blood flow during the first 100 minutes of NMP. Fit lines for linearity are added.

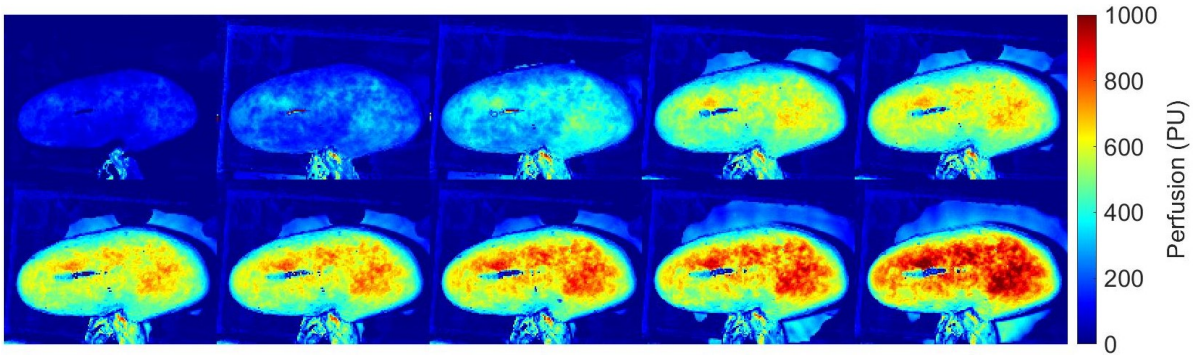

(a) Kidney 1

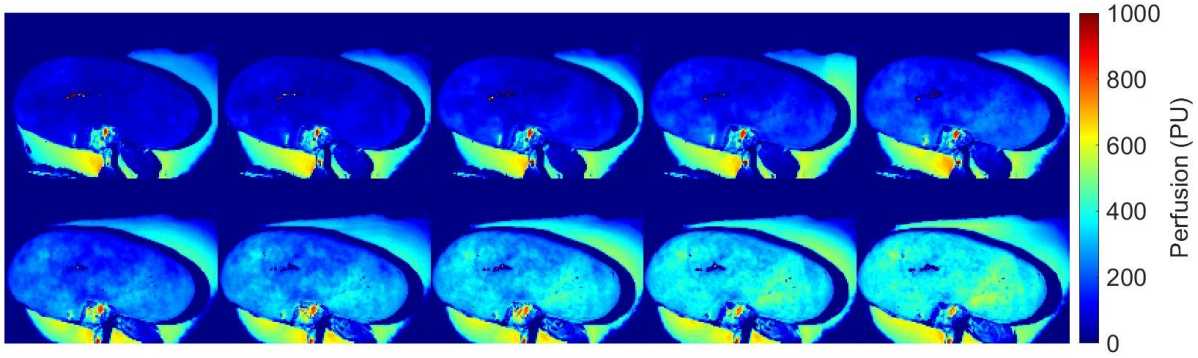

(b) Kidney 2

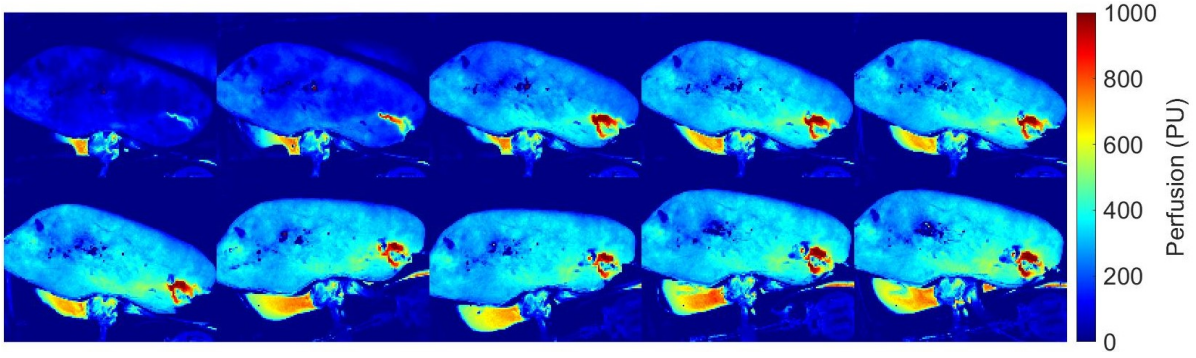

(c) Kidney 3

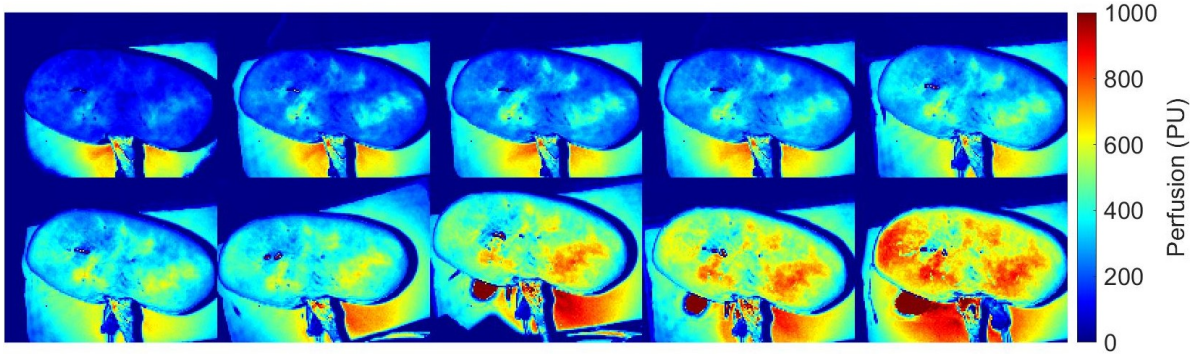

(d) Kidney 4

Figure 2.18: Perfusion of the four kidneys during the first 100 minutes of NMP. The top row of each subfigure consists of perfusion images of the 10, 20, 30, 40, and 50 minute time intervals and the bottom row consists of perfusion images of the 60, 70, 80, 90, and 100 minute time intervals.

Furthermore, it is noticeable that kidneys 2 and 4 have a relatively constant increasing flow. Meanwhile, kidneys 1 and 3 assume a constant flow around 40 minutes after the start of the NMP. The total flow also differs per kidney. Kidney 4 achieves a much higher flow after 100 minutes of NMP than the other kidneys.

The rate of increase in perfusion varies between the kidneys. In kidneys 1 and 4, the perfusion increases more rapidly than in kidneys 2 and 3. Also, the maximum perfusion after 100 minutes of NMP is much higher.

Similar to the LSCI data from the different positions, in all images, it is noticeable that the perfusion decreases towards the edge of the kidney. Further, the images have dark blue spots, mainly at the same position. In kidney 3, an increasing red spot is present. This is due to a bleed on the surface caused by taking a biopt.

2.3.3. Perfusion for different angles of incidence

After the recordings of the kidney placed in different positions and observed over time, more recordings were made of position 1. The angle of incidence of the LSCI device was adjusted. Starting with a perpendicular angle of incidence of 0° and ending, after steps of 10°, at 40°. The mean perfusion of the observed ROI is calculated for three kidneys at every angle of incidence. No measurements for different angles of incidence were performed on kidney 1.

The arterial flow from each measurement is given in Table 2.2. In kidneys 2 and 3, the flow during the measurements is relatively equal (ranging between 100 and 113 mL/min and between 106 and 107 mL/min). However, the flow in kidney 4 differs significantly per measurement (ranging between 129 and 182 mL/min). Section 2.3.2 indicates a linear correlation between the flow and perfusion values. Therefore Figure 2.19 shows the perfusion versus the angle of incidence, and Figure 2.20 shows the perfusion divided by the flow versus the angle of incidence.

Arterial flow (mL/min)	0°	10°	20°	30°	40°
Kidney 2	100	103	107	110	113
Kidney 3	107	107	106	106	106
Kidney 4	129	147	161	170	182

Table 2.2: Arterial flow (mL/min) during each measurement of three kidneys using five different angles of incidence.

The measured perfusion decreased for larger angles of incidence. At an angle of 40°, an average decrease of 14% was observed. However, in kidney 4, the difference in perfusion between angle 0° and angle 40° is much smaller than in kidneys 2 and 3. The variation of perfusion between 0° and 10° is 1.1%, between 0° and 20° 0.43%, and between 0° and 30° 5.6%. When dividing the measured perfusion by the arterial flow, a decrease of 27% was observed between 0° and 40°. The variation between 0° and 10° is 3.6%, between 0° and 20° 10%, and between 0° and 30° 17%.

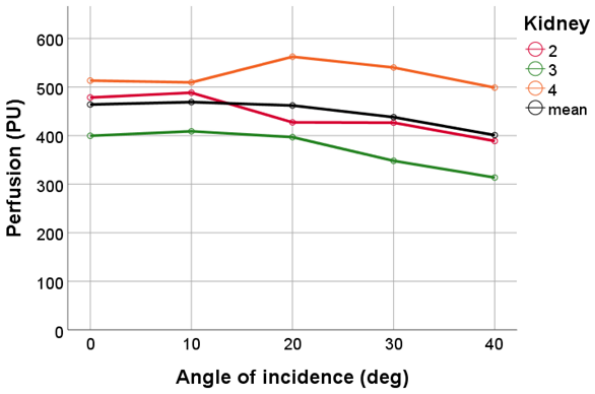

Figure 2.19: Mean perfusion of the ROI per angle of incidence.

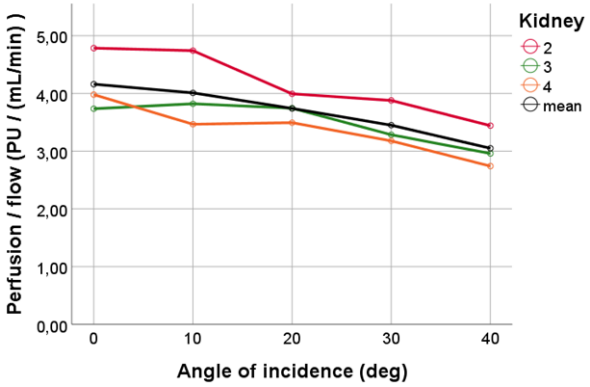

Figure 2.20: Mean perfusion of the ROI divided by arterial blood flow per angle of incidence

2.4. Discussion

2.4.1. Perfusion in different positions

The setup and method designed to obtain 2D perfusion recordings of the kidney made it possible to image each side of the kidney and obtain data from the vast majority of the surface of each kidney. The shape and size of the kidneys were very diverse, resulting in different outcomes between kidneys.

Positioning the kidney in positions 1 and 2 presented no problems, as well as placing the kidney in positions 3 and 4. However, kidney 3 (the most significant size kidney) just fitted the 3D-printed model for positions 3 and 4. It is necessary to have a 3D-printed model with increased dimensions for kidneys of a larger size than kidney 3 to prevent damage to the kidney's surface by the 3D-printed model. In positions 5 and 6, some kidneys could not stay in the upright position. For these kidneys, the 3D-printed model for positions 3 and 4 was used to keep the kidneys balanced. By changing the position of the kidney, in some cases, the arterial flow decreased drastically. This was due to kinking of the tubing or the artery. However, this could be solved quickly by repositioning the tubing or artery. In position 3, this problem was more common because of the artery overlaying the 3D-printed model due to gravity. The 3D-printed model can be improved by making a support for the tubing. Repositioning the kidney also resulted in (red) perfusion fluid being spread over the surface of the kidney. This problem can be solved by cannulating the renal vein, allowing blood to flow directly into the reservoir.

Within the kidneys, the flow differs per position in some cases. For example, the flow is often higher in positions 1 and 2 than in positions 5 and 6. The cause of this is unknown, but gravity may play a role here. It can be tested whether the order of the positions is essential. Measurements were performed in order from position 1 to 6 as standard, but this could also be alternated. Furthermore, it can be tested whether imaging the positions by holding the camera horizontally on the surface makes a difference in measured perfusion. If the flow remains the same horizontally and vertically, it can be examined whether gravity influences the perfusion in the kidney. The other settings of the moorO_2Flo must stay the same.

The size of the kidney was a limiting factor. Kidney 3 did not entirely fit the FOV in positions 1-4; therefore, no perfusion data from the sides of the kidney could be obtained. This limitation was related to the setup of the LSCI device. The moorO_2Flo was attached to an arm that was adjustable in height. However, this height was limited, so the maximum distance of 380 mm could not be reached. The kidney fit the maximum FOV of 150 by 200 mm; therefore, imaging of the kidney would have been possible if the moorO_2Flo had more freedom of movement.

Perfusion decreased towards the edge of all kidneys in all recordings. This is the result of the kidney's convex surface, and the effect is increased for larger angles of incidence. In positions 5 and 6, most of the surface has an angle of incidence >0°. In positions 1 and 2, the effect was on a relatively small area. Results of the influence of the angle of incidence should be applied in the 3D visualization because of the unreliable data at the edges. The arcs with deviating perfusion arise from the kidney's shape and mark the renal hilum's boundary. Below the arc is the bottom of the kidney belonging to the part below the renal hilum. In the arc region, the incidence angle is very high, resulting in a decreased measured perfusion.

When comparing the perfusion data within a single kidney across the positions, it is noticeable that the measured perfusion in positions 5 and 6 is higher compared to other positions. The gain settings cause this problem. The gain was set in advance based on position 1 and has not been adjusted for every experiment when the position was changed. The gain settings also caused artifacts with reduced perfusion (dark blue spots) on the LSCI recordings. Artifacts occurred at locations where the intensity was too high. The gain was set automatically to the most optimal settings, but this could not prevent the artifacts.

Results before and after clamping clearly show the areas with and without ischemia. By comparing the ischemia distribution between the kidneys, it can be seen that ischemia is not always visible in the recording of every position. Looking at the perfusion data of a single position can indicate that no

ischemia is present (kidney 4 in position 2), whereas other positions of the kidney clearly do indicate the presence of ischemia. This proves that it is necessary to look at all sides of the kidney, or ischemia may be missed.

With the designed method and setup, it was possible to obtain 2D perfusion recordings of the entire surface of the kidney. Adjusting the LSCI setup will solve the FOV problem. To be able to use the data for the 3D visualization, the unreliable data around the edges of the kidney due to the convex surface should be compensated.

2.4.2. Perfusion and flow over time

The results of the flow and perfusion over time show that there is a strong linear correlation. The results from kidney 3 confirm this strong correlation between the flow and the measured perfusion due to the many data points close to each other. However, the correlation differs per kidney. After 100 minutes of NMP, kidney 4 has the highest flow but not the highest perfusion. The reverse is the case with kidney 2. After 100 minutes of NMP, the kidney has the lowest flow, but the perfusion is not the lowest. It can therefore be concluded from the results that the measured perfusion can only be viewed per kidney and that a comparison with other kidneys is not a reliable situation due to the relative value of the perfusion.

The difference in the flow development for the different kidneys is striking. Kidneys 2 and 4 show a similar development because the flow continues to increase over time. In kidneys 1 and 3, the flow levels stabilize after about 40 minutes. This difference can possibly be explained by the time of the experiment. The experiments of kidneys 1 and 3 were performed the day the kidneys were collected from the slaughterhouse. The experiments of kidneys 2 and 4 were performed the day after. In the meantime, the kidneys have been on HMP for 24 hours. Kidneys 1 and 3 were connected to HMP for a much shorter time. However, it needs to be clarified what the desired pattern of flow and perfusion development is. Many NMP studies assume a higher flow is better. Hosgood et al. (2015) developed a scoring system for the pretransplant assessment of kidney quality. Kidneys with a flow > 50 ml/min/100 grams were assigned a better score than kidneys with a flow < 50 ml/min/100 grams [18]. However, the flow will also have to stabilize over time because if it continues to increase, this could be caused by kidney damage. Regulation of the renal resistance may be damaged, resulting in increased flow, but in the meantime, the kidney's function is reduced. To be able to make a reasonable assessment based on flow and perfusion, other biomarkers, such as renal clearance function, will always have to be considered.

2.4.3. Perfusion for different angles of incidence

The results show that the measured perfusion decreases for an increased angle of incidence. However, interpreting the data was difficult because the circumstances were different for each kidney. Flow differed per kidney and angle of incidence measurement. In kidneys 2 and 3, the flow was constant over the angles of incidence. However, in kidney 4, the flow still increased during the experiment resulting in different flow values for the increasing angles of incidence. A better comparison could be made by dividing the measured perfusion by the flow. Flow should be kept at a constant value to prevent this. Furthermore, since only three kidneys were used for the experiment, the obtained data set was minimal. It is recommended to repeat the experiment with more kidneys to have a more extensive data set to get more reliable results.

In two recordings (kidney 2 at 20° and kidney 4 at 40°), a gray area was present where no perfusion could be measured. Figure 2.21 shows the perfusion image with the gray area for kidney 2 at 20°. The ROI did not include part of the gray area. Therefore the results were not influenced. In the gray area, the angle of incidence was larger than 20°. These results show that the LSCI device itself also has problems with larger angles of incidence. However, this problem did not occur when making the LSCI recordings of the six different positions.

The decrease of the measured perfusion for an increased angle of incidence corresponds with the expectations and with the LSCI data of the six positions where the perfusion decreases towards the edges of the kidneys due to an increasing angle of incidence.

No research has been done into measured perfusion at angles of incidence above 40°, but it is expected that the perfusion will only decrease more. Therefore, before using the perfusion data from the six positions for the 3D visualization, it is recommended to remove perfusion data measured at places where the angle of incidence is >40°. The measured perfusion at these locations is much lower than it should be and, therefore, unreliable.

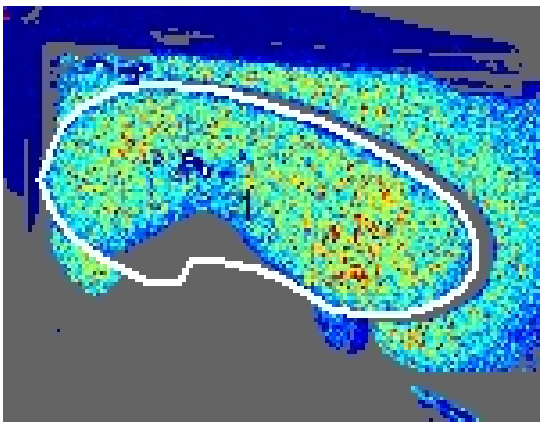

Figure 2.21: Perfusion image for kidney 2 at 20°. Part of the perfusion on the surface of the kidney could not be visualized and is presented as a gray area. The white ROI is the contour of the kidney.

3

Three-dimensional visualization of renal microcirculation

This chapter describes the process of modeling the 3D visualization of the renal microcirculation using a 3D model of the kidney combined with perfusion data collected with the laser speckle contrast imager. The method is based on the knowledge gained in Chapter 2. First, an introduction is given about 3D imaging methods. Next, the methods for constructing the 3D kidney model and the 3D perfusion model are described, and the results are given and discussed.

3.1. Introduction

Two types of data are needed to achieve a 3D visualization of the microcirculation: 3D data of the object to be visualized and 2D data of the perfusion. The 2D data of the perfusion over the entire surface is obtained with the laser speckle contrast imager by placing the kidney in multiple positions. 3D data of the kidney can be obtained by applying a 3D imaging method. The 3D kidney data is needed to give depth to the 2D perfusion data.

It is desirable to obtain 3D data and make a matching 3D model of every kidney. The method for creating the 3D model should be simple and fast so that it can be performed during the NMP procedure. This limited period of time should allow the perfusion quality of the kidney to be assessed before the kidney is transplanted to the recipient.

Constructing a 3D model of an object is possible using 3D imaging. Different imaging methods can collect 3D data of the object, which will be constructed into a computer model. 3D imaging can be divided into two main categories: contact and non-contact imaging. Contact imaging is a slow method where the object is touched spot by spot to map each location. Non-contact imaging is generally faster but can also be more complicated.

Three possible 3D imaging methods were considered for making the 3D model of the kidney: CT scanning, time-of-flight principle, and shape from silhouettes. The working principles of these methods and their advantages and disadvantages are explained.

CT-scanning

CT scanning is a medical imaging technique that uses X-ray. The method is widely used to create internal images of the body. The object-to-image is placed in an X-ray tube. Then several measurement tasks from different angles are performed. Cross-sections of the object are produced using the results. These cross-sections together form a 3D model of the object [5]. A CT scanner is present in the Erasmus MC and available for imaging animals and animal organs. The advantages of this method are the high resolution of the 3D model, the possibility to view the kidney's internal (vascular) structure, and the processing of the data is fast and automatic with the software of the device. The disadvantages are that the scan takes a few minutes, during which time the kidney undergoes warm ischemia. In addition,

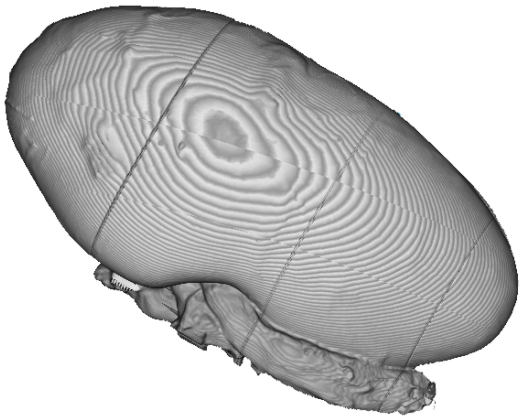

Figure 3.1: 3D model of a porcine kidney made using CT-scanning.

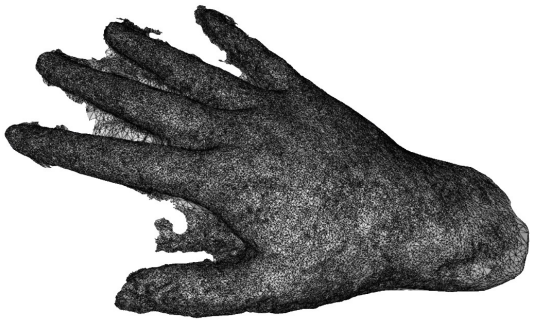

Figure 3.2: 3D model of part of the hand using the time-of-flight principle.

the kidney is exposed to radiation, and the purchase and use of a CT device are costly. Further, when using the available CT scanner, multiple scans of the kidney must be taken and combined to make one 3D model. This is because the kidney is too large for the device's maximum object size. Figure 3.1 shows a 3D model of a porcine kidney made using the CT scanner.

Time-of-flight principle
Time-of-flight is an active imaging technique that determines distances based on the time it takes for light to hit an object and return to the camera. The distance d can be determined by the formula $d = (c * t)/2$ where c is the speed of light and t the measured time [14]. Various smartphones have a Time-of-Flight camera. The method's advantages are that it is easy to apply and quick to implement. The resolution is also high. The disadvantage is the time it takes to collect a data set. Further, at least two measurements should be performed to model both sides of the kidney. The method is tested using the app 3D Live scanner for Android (Lubos Vonasek Programmierung). It was possible to obtain a high-resolution model of a part of the hand (Figure 3.2). However, modeling the kidney did not work because there were problems due to the reflective surface of the kidney.

Shape from silhouettes
Shape from silhouettes is a method that can reconstruct a 3D model from 2D silhouette images of the object. Three or more silhouettes/contours are extracted and overlapped based on their known orientation. This overlapping can create a 3D voxel grid containing 3D data of the object [26]. The advantages of the method are that it is easy to use, it is passive because no specific light/radiation source is required, silhouettes can be obtained during NMP so that there is no extra warm ischemia, the method is fast, and it is cheap because no additional equipment is required. The disadvantage of the method is that the resolution is low, which means that detail in the structure of the kidney is missing in the 3D model.

Ultimately, the method shape from silhouettes was chosen to continue working with. The method is easy to apply and fast and requires no additional equipment. Despite the lower quality of the model compared to other 3D imaging methods, this is not a reason to reject the method. The perfusion model should provide insight into the overall distribution of the perfusion. The exact location of perfusion deviations is of less importance.

Combining the 3D model with the 2D perfusion images reconstructs the 3D perfusion model. The perfusion (with the degree visible based on a range of colors) on the model must correspond to the location of the corresponding perfusion image taken. Since the perfusion images are taken at varying flows, this should be considered. Further, the perfusion over the kidney is deviated by the angle of incidence over the convex surface. This should also be taken into account when creating the perfusion model.

3.2. Method

3.2.1. Three-dimensional kidney model

The 3D model of the kidney is constructed using the 3D imaging method shape from silhouettes. Three silhouettes are used. These are the contours of the kidney seen from the three body planes (sagittal, horizontal, and frontal plane). The contours are observed from above when the kidney is placed in position 1, position 4, and position 5. The contour of position 1 is in the yz-plane of the 3D model, the contour of position 4 in the xz-plane, and the contour of position 5 in the xy-plane.

Data for the silhouettes are obtained from the LSCI recordings. The recordings of the kidney in positions 1, 4, and 5 are used. The method of the experiment to get the perfusion recordings is explained in Section 2.2. Frame 1 of each recording is exported to an RGB image with a resolution of 580 by 572 pixels. Contours of all positions are labeled and exported to .png files.

MATLAB (MathWorks, Inc.) is used to construct the 3D model with the three contours. Loading the .png files in the MATLAB workspace by imread results in 2D logical arrays in which the kidney contour is assigned value 1 and the background value 0. The contour arrays are cropped to the edges of the contours by removing rows and columns containing zeros only. The three remaining contours are not proportional. Therefore the ratio between the contours is needed. The kidney's width, length, and depth (in pixels) are read from the contours. After this, the ratio between them is calculated. Based on these ratios, the contours are resized to become proportional. Figure 3.3 shows a schematic overview of processing the three contours.

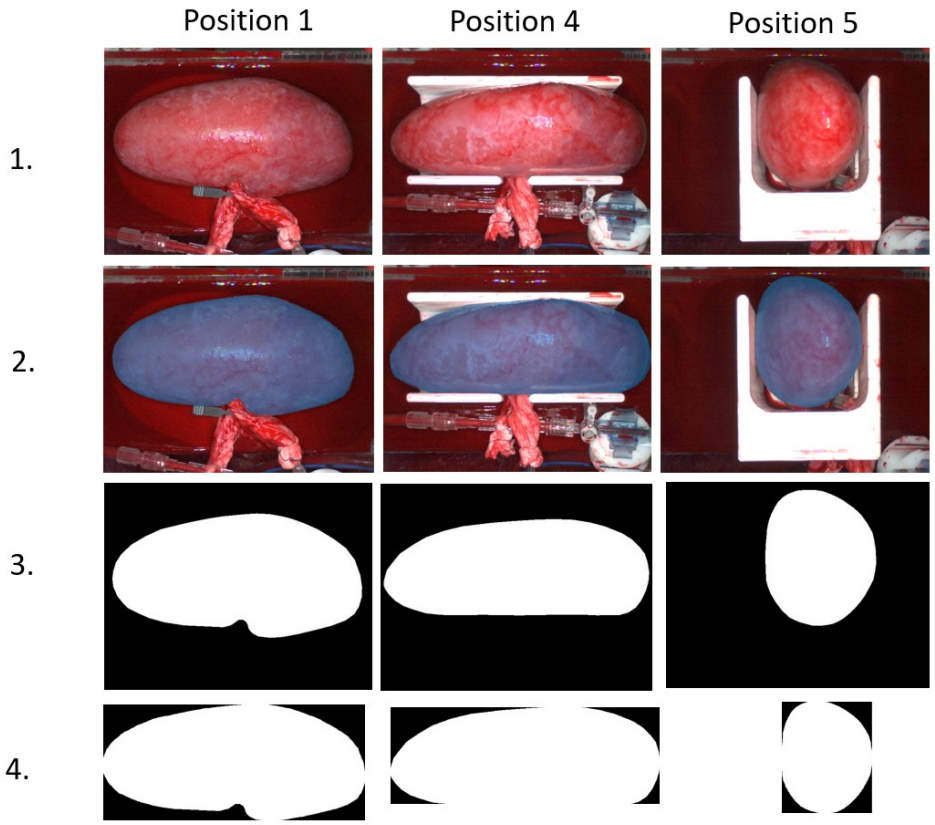

Figure 3.3: Stepwise process of contour generation. First, frame 1 of the LSCI recordings of positions 1, 4, and 5 are exported to RGB files (1). Then the contours are labeled (2). The contours are imported in MATLAB and converted to logical arrays (3). Lastly, the arrays are cropped and resized to become proportional (4).

After finishing the contours, the 3D model is created in a 3D logical array (array consisting of ones and zeros only). The three contours are superimposed and overlapped on the horizontal, frontal, and sagittal planes. The 3D coordinates with an overlap of all three contours are assigned the value 1. The

other locations are assigned the value 0. This generates a 3D grid of cubes, with each cube having a coordinate (x,y,z). The 3D grid is visualized using the MATLAB app VolumeViewer. Figure 3.4 provides a schematic overview of the construction of the 3D model of the kidney. Due to the limited data with only three contours, making the 3D model smoother is desirable. For this, the shape of the contours is interpolated over the corresponding plane.

The MATLAB code created for programming the 3D model of the kidney is included in Appendix D. The code can be used for any kidney, the input: the three contours will have to be renewed per kidney. The 3D model is stored as a logical 3D array in a .mat file.

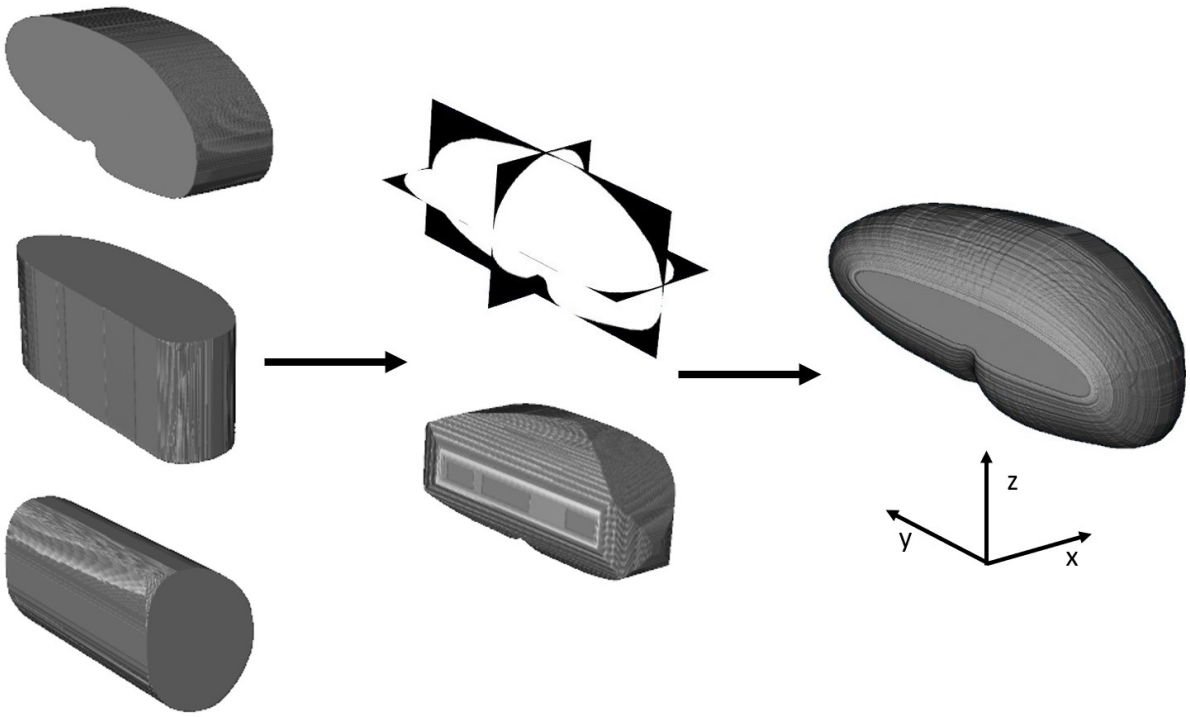

Figure 3.4: Schematic overview of 3D model reconstruction from contours to 3D grid model. First, depth is given to the three contours. Then the three models are overlapped on the three planes. Coordinates without overlap are assigned the value 0, and coordinates with overlap are assigned the value 1. Lastly, the model is smoothed by interpolating the shape of the contour over the corresponding plane.

3.2.2. Three-dimensional perfusion model

The 3D perfusion model is made by combining 2D perfusion data with the 3D model of the kidney. The method is based on assigning depth to the 2D perfusion images and is explained below. The corresponding MATLAB code is attached in Appendix E. The input for the perfusion model consists of the following:

- 3D array of the 3D model of the kidney
- 2D arrays of the perfusion data for each position
- Contour images for each position
- Length of the kidney (read from the moorO_2Flo)
- Distance between the moorO_2Flo and the kidney (read from the moorO_2Flo)

Changing the input data for different kidneys and the situation before or after clamping can create a perfusion model for each case.

Preprocessing of the perfusion data
The first step is to preprocess the perfusion images. Mean perfusion images of the six positions are used. The method for obtaining these .mat files is given in Subsection 2.3.1. For each perfusion image, a corresponding contour image is needed. Similar to Subsection 3.2.1, the contours of each position are labeled with MATLAB image labeler. The contour labels are exported to .png files and loaded in the MATLAB workspace. Next, the contours are resized to 116 by 150 arrays and are superimposed on the perfusion images to remove perfusion data corresponding to the background. This results in perfusion images containing perfusion data from the contour only. After this, the perfusion files are cropped to the edges of the contours by deleting rows and columns consisting of zeros only.

Assigning depth to the perfusion data
Perfusion data is given depth using the 3D model of the kidney. Perfusion data of each position is resized to the ratio of the kidney in the 3D model. A 2D array of the depth of each coordinate of the position is created. The 2D perfusion array is overlapped on the corresponding plane of the 3D model. A value for the depth is assigned if the overlap has a 1 in the logical 3D array of the 3D model for the corresponding 2D coordinate.

Determine the angle of incidence over the surface of the kidney
Due to the influence of the angle of incidence on the measured perfusion, perfusion data obtained at an angle of incidence >40° is considered unreliable. Therefore this data is discarded. For each position (1-6), a model is made that calculates the angle of incidence for each pixel on the surface. The angle of incidence is the angle between the laser input on a certain point of incidence (vector $\vec{B}$) and the normal of this point of incidence (vector $\vec{A}$). Figure 3.5 shows the vectors and angle of incidence schematically. Two coordinates are needed to determine the angle of incidence: the coordinate of the incidence point and the coordinate of the moorO_2Flo. The angle of incidence (θ) between the two vectors is calculated using the following equation:

$$\theta = \cos^{-1} \frac{\vec{A} \cdot \vec{B}}{|A| \cdot |B|} \tag{3.1}$$

For the vector from the moorO_2Flo to the incidence point, the distance between the moorO_2Flo and the kidney is needed. The distance (in mm) can be read from the corresponding perfusion file in the moorO_2Flo software. The distance is converted to pixels by the ratio of the length of the kidney. The length of the kidney (in mm) is measured in the moorO_2Flo software by assigning a line over the length. The corresponding pixel value is known. The normal vector of each incident coordinate is determined in MATLAB using the surfnorm function. This function creates a vector normal to the surface for each coordinate. The angle of incidence of each pixel per position is calculated using Equation 3.1 and stored in a 2D array.

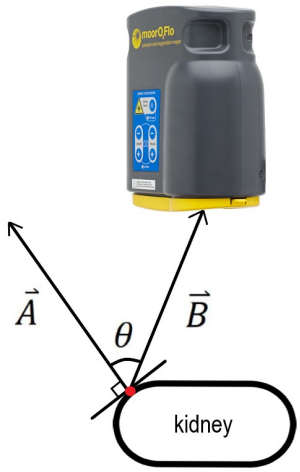

Figure 3.5: The angle of incidence (θ) from the moorO_2Flo on the kidney. The angle of incidence is the angle between the two vectors. Vector A is directed normal from the kidney surface at the point of incidence (red dot). Vector B is directed from the point of incidence to the moorO_2Flo, representing the line of the laser.

Creating the 3D visualization using a point cloud
After preprocessing the perfusion data, assigning depth to the perfusion data, and making the angle of incidence models, a point cloud is made. In the point cloud, each point represents a 3D coordinate based on the 2D coordinate in the contour of the position and the corresponding depth of the 3D model. The point is assigned a color based on the perfusion value. The RGB color depends on the perfusion value, which is in the range of 0 to 1000 PU. The 'jet' colorbar consisting of 256 colors is used. A point is generated if the angle of incidence from the 3D coordinate is ≤40°. The point cloud is saved as a .ply file and can be visualized in MeshLab (Visual Computing Lab, ISTI - CNR). Combining the points of the six positions results in the 3D visualization of the renal microcirculation. For some coordinates, there is an overlap in data points because the perfusion of a particular coordinate has been measured in two or more LSCI recordings. If this is the case, the overlapping data points are compared by perfusion value, and only the data point with the highest perfusion value is left. The remaining points have been removed. If the data point has been removed due to an angle of incidence >40°, this is filled with a white point to show that no reliable perfusion value has been measured for the coordinate concerned. Figure 3.6 shows a schematic overview of the method, from obtaining the 2D perfusion data to displaying the 3D perfusion model as a point cloud.

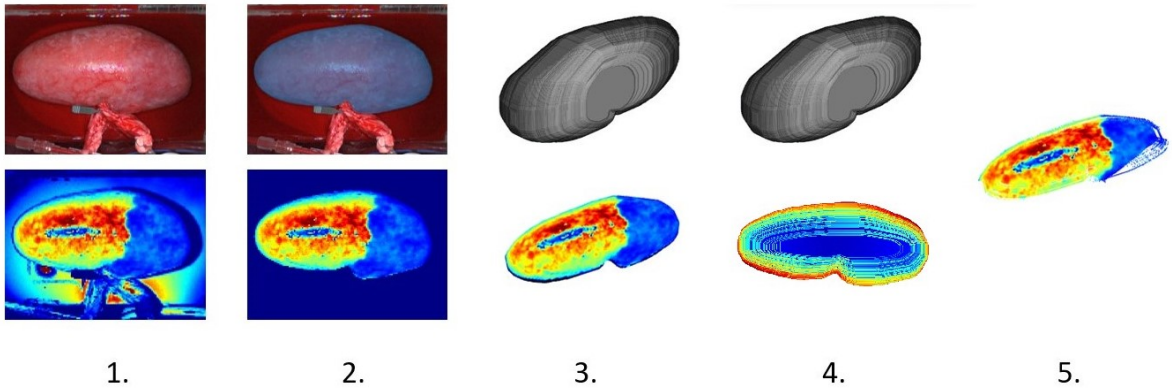

Figure 3.6: Schematic overview of 3D perfusion model reconstruction for position 1. Starting with the color and perfusion image of the position (1). Then the contour is selected using MATLAB image labeler, and the contour is overlapped on the perfusion image to remove the background perfusion (2). The 3D model of the kidney is used to assign depth to the perfusion image, and a point cloud is created (3). Using the 3D model of the kidney, the angle of incidence is determined over the surface (4). Lastly, the point cloud is compensated for the angle of incidence by removing perfusion data belonging to angles of incidence >40° (5).

3.3. Results

3.3.1. Three-dimensional kidney model

LSCI data was collected from four porcine kidneys, similar to the kidneys from Chapter 2. Eight 3D models were created: two 3D models per kidney. One model uses the data before clamping the inferior branch of the artery, and one uses the data after clamping. Figure 3.8 shows the 3D models.

The models before and after clamping should be similar since the appearance of the kidney, except for a few color differences due to ischemia, does not change. For kidneys 1, 2, and 4, the models before and after clamping are largely the same. However, in kidney 3, there is a clear difference. This is due to the contours of the kidney. The contours of all kidneys are inserted in Figure 3.7. In positions 1 and 4, kidney 3 is not entirely in the FOV resulting in cut edges. Also, the contour of position 5 is oriented differently compared to position 5 before clamping. Therefore, when comparing the contours before and after clamping, there is mainly a difference in the contour of position 5, where the shape deviates more from positions 1 and 4. The contours of positions 1 and 4 hardly differ.

Models do not contain 3D data of the artery, vein, and ureter. Furthermore, the accuracy around the renal hilum is low due to the lack of data from this location. Interpolating over the contour shape makes the renal hilum seem more prominent in the 3D model than it is in the real kidney. The size of the renal hilum differs per kidney.

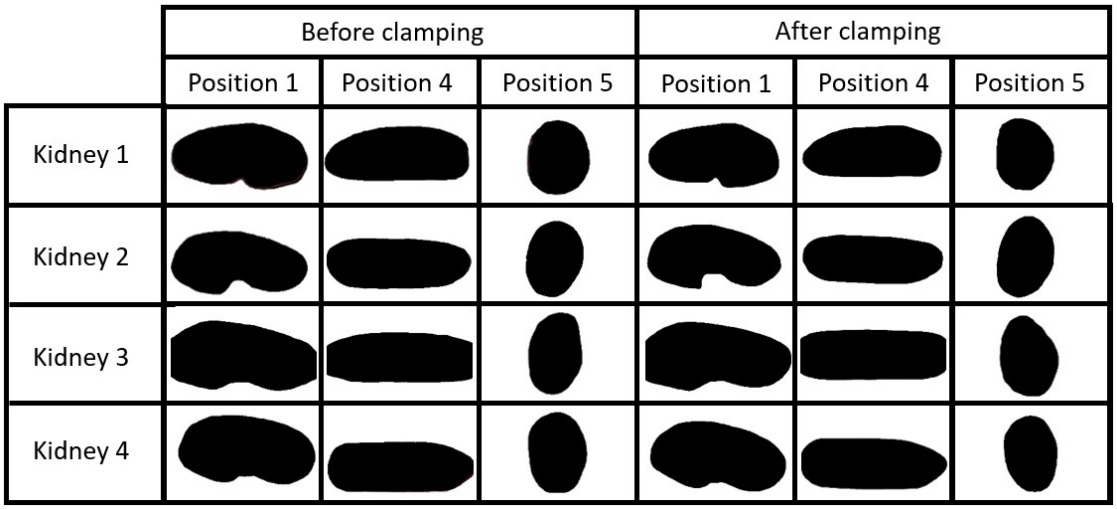

Figure 3.7: Contours of positions 1, 4, and 5 of the four kidneys both before and after clamping the inferior branch of the artery.

The contour figures of position 4 show that the top and bottom of the contour are flattened by using the 3D-printed block to hold the kidney in place. However, this is not noticeable in the contours of position 5.

The contour of position 1 of kidney 1 is mirrored concerning the other kidneys. This is a property of the kidney and not an error in the measurement.

From the moment the LSCI data is obtained, it takes a maximum of 10 minutes to get a complete 3D model of the kidney. Most of the time is spent exporting and loading the data into MATLAB and manually selecting the contour.

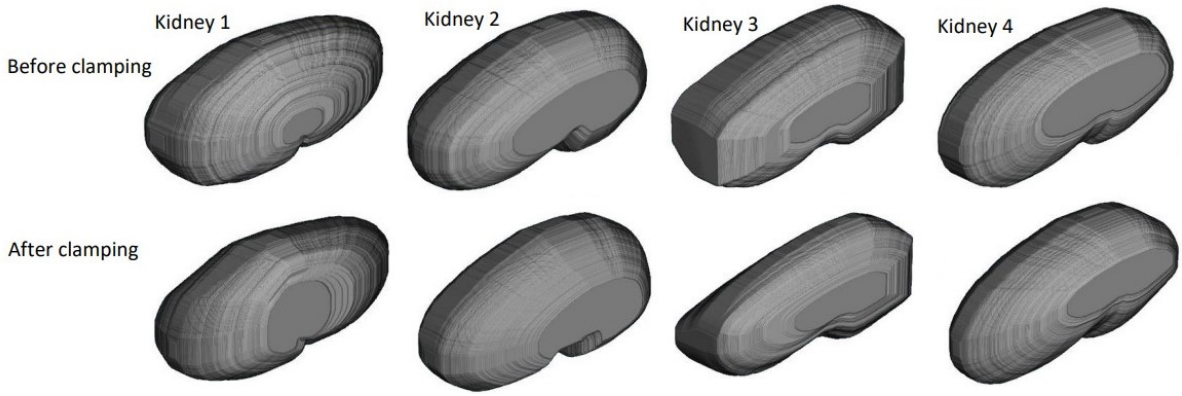

Figure 3.8: 3D models of the four kidneys before and after clamping the interior branch of the artery.

3.3.2. Three-dimensional perfusion model

By using the 3D models from Subsection 3.3.1 and the perfusion data from the six positions from Subsection 2.3.1, the method for making the perfusion models could be performed for all four kidneys. Eight 3D perfusion models were made. For each kidney, one by using the data before clamping and one by using the data after clamping. For each kidney, the angle of incidence was determined over the entire surface. The 3D visualization was optimized using this data. First, the results regarding the angle of incidence will be given. Then, the perfusion results before and after clamping the artery are provided and compared to validate the perfusion model.

Angle of incidence

The relationship between the angle of incidence and the measured perfusion values indicates that LSCI data measured with an angle of incidence >40° is unreliable. Therefore, the perfusion data measured at coordinates with an angle of incidence >40° are removed. For this, the angle of incidence of each coordinate is calculated. Figure 3.9 shows the angle of incidence over the surface of the six positions of kidney 1 (before clamping). Perfusion images of the corresponding positions are also included in the figure to compare the perfusion and angle of incidence.

The results show that the perfusion model is in line with expectations. It is clearly visible that the angle of incidence decreases towards the edge of the kidney. Around the edge, the angle of incidence is 90°. Positions 1 and 2 have the largest surface with an angle of incidence ≤40°. This area is already smaller in positions 3 and 4, and at positions 5 and 6, there is only a small part of the kidney with an angle of incidence ≤40°. This corresponds to the expectation because the kidney is upright in positions 5 and 6, resulting in a more convex shape.

In position 3, the increase in the angle of incidence at the renal hilum is clearly visible. Further, in position 6, there is a line with a lower angle of incidence at the bottom of the figure. This is where the lower widening of the kidney begins (below the renal hilum). Furthermore, it is visible (particularly in positions 2 and 4) that the angle of incidence does not gradually increase in the model (from the center to the edges) even though the slope of the actual kidneys surface does increase smoothly.

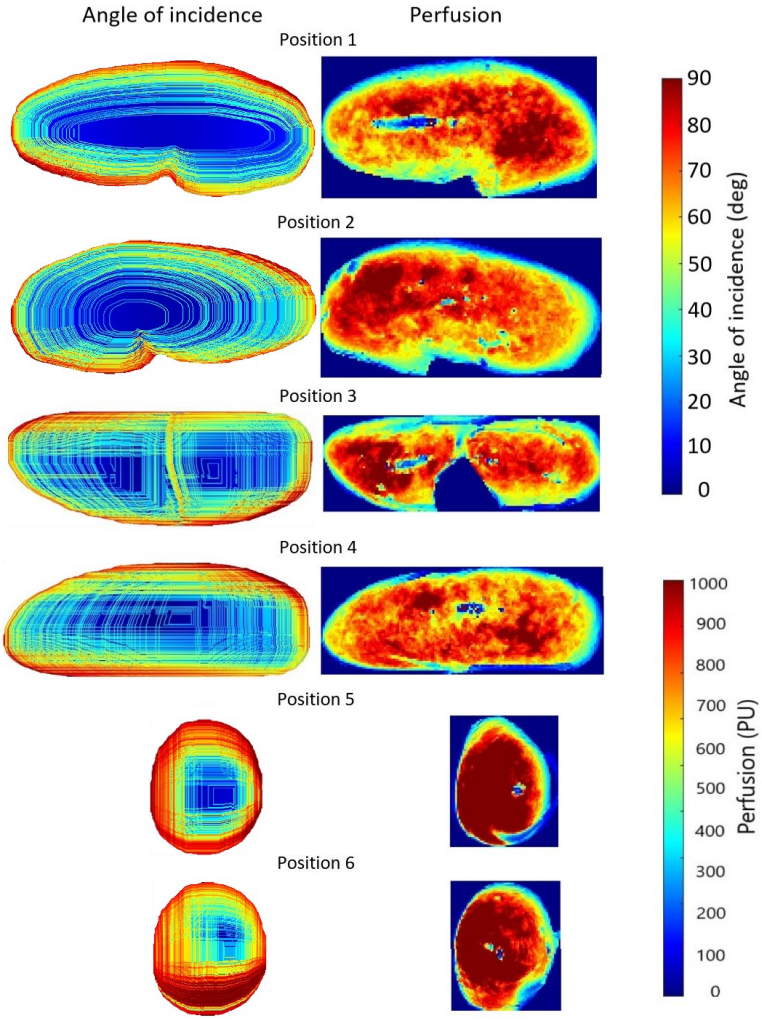

Figure 3.9: Angle of incidence and measured perfusion of kidney 1 for six positions.

Perfusion model with and without angle of incidence compensation
Figure 3.10 shows the point clouds containing the 3D perfusion models of kidney 1. The left figures include the perfusion models without compensation for the angle of incidence. The figures on the right are the models with compensation for the angle of incidence where data points with an angle of incidence >40° have been removed. This results in a better overlap of perfusion values. Furthermore, low perfusion values associated with the edges of the kidney and the background are removed. This also results in less overlap of points. However, by removing these points, there are also some locations on the surface of the kidney without data points. These locations are indicated with white-colored points to show that these points have no reliable perfusion data. Lastly, overlapping data points are compared on their perfusion value. The data points with the highest perfusion value remained.

The model after compensation still contains some data points with a lower perfusion value than expected. This is more noticeable in the model before clamping than after clamping because the perfusion values are already lower in the model after clamping due to ischemia.

In positions 5 and 6, the overall perfusion values are higher. In the model with compensation for the angle of incidence, this is more visible due to the removal of surrounding and overlying data points from the other positions.

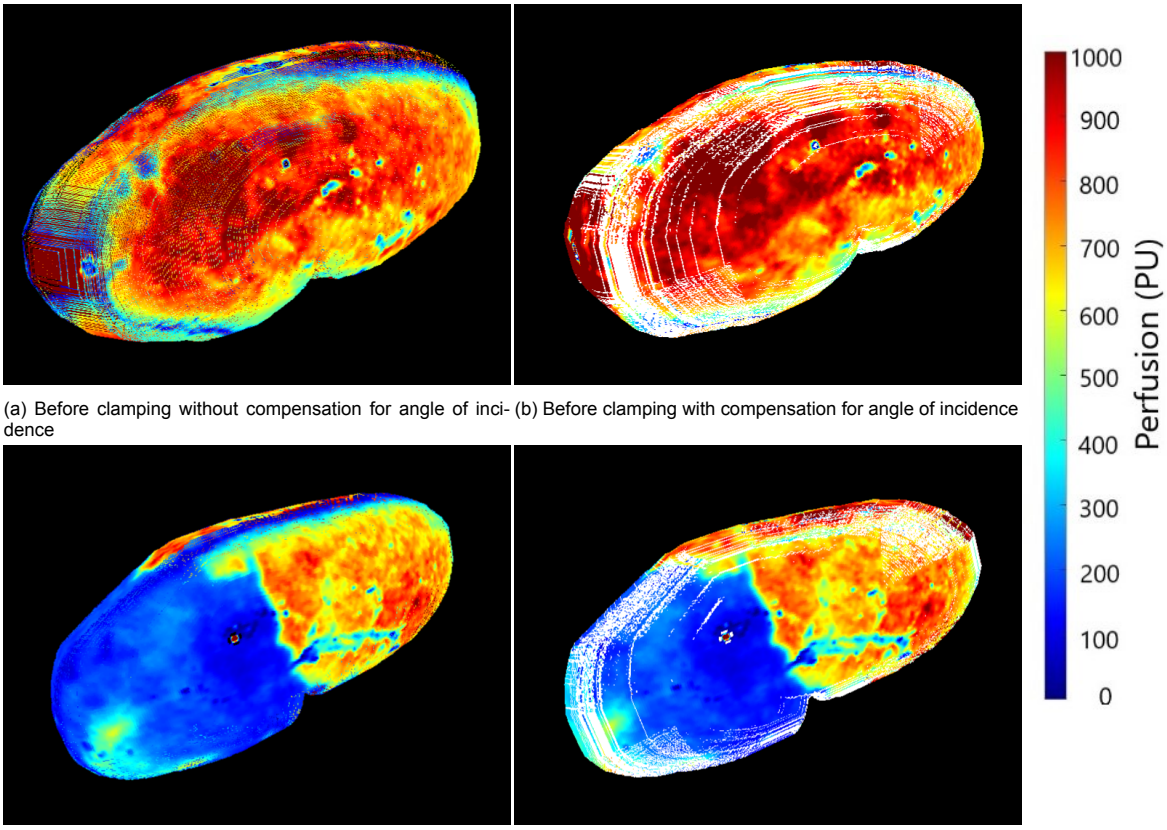

(a) Before clamping without compensation for angle of incidence

(b) Before clamping with compensation for angle of incidence

(c) After clamping without compensation for angle of incidence

(d) After clamping with compensation for angle of incidence

Figure 3.10: 3D perfusion models for kidney 1 in four situation: before / after clamping and with / without compensation for the angle of incidence.

Perfusion model before and after clamping
To verify the functioning of the model, data was collected from each kidney during normal perfusion and perfusion under ischemia caused by the clamping of a branch of the artery. Both perfusion models of kidney 1 are shown in Figure 3.10. When comparing the models, it is clear that the perfusion after clamping is reduced on the inferior side of the kidney. The model clearly shows where the ischemia is and is not present. In kidneys 1, 2, and 4, ischemia was evenly distributed over the inferior side of

the kidney. Ischemia was observed in position 1 as well as in positions 2, 3, 4, and 6. However, this was not the case in the experiment with kidney 4. In kidney 4, it is noticeable in the perfusion model that ischemia did not occur over the entire inferior side of the kidney during the artery clamping. This is shown in Figure 3.11. Ischemia is only present on one side of the kidney (ischemia is visible in positions 1, 3, 4, and 6, but not in position 2). This indicates that the blood vessel structure differs per kidney.

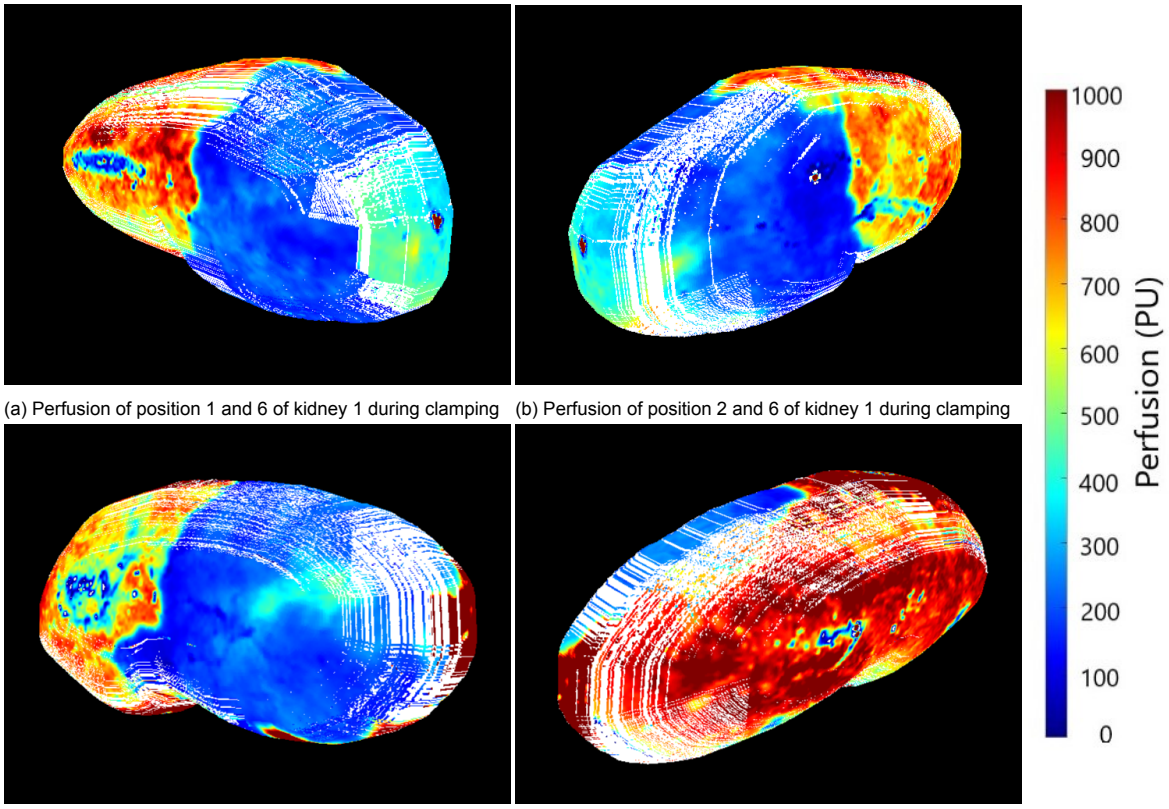

(a) Perfusion of position 1 and 6 of kidney 1 during clamping

(b) Perfusion of position 2 and 6 of kidney 1 during clamping

(c) Perfusion of position 1 and 6 of kidney 4 during clamping

(d) Perfusion of position 2 and 6 of kidney 4 during clamping

Figure 3.11: Perfusion in kidneys 1 and 4 during clamping. Clamping does result in ischemia over the entire inferior side of kidney 1, but this is not the case in kidney 4. In position 1 of kidneys 1 (a) and 4 (c) ischemia is visible, but in position 2 ischemia is only present in kidney 1 (b). No ischemia is present in position 2 of kidney 4 (d).

3.4. Discussion

3.4.1. Three-dimensional kidney model

The 3D models give a clear picture of the natural shape and sizes of the kidneys. Moreover, due to simple operation, a model can be made quickly of each kidney in every situation. It is beneficial to create a new model for each kidney since the models indicate that the kidneys differ significantly in shape and size. For example, kidney 3 was much larger than the other kidneys, and kidney 1 was mirrored in shape.

The quality of the 3D model depends on the quality of the obtained contours. The contours of position 1 were the most natural to achieve due to the kidney lying in this position without assistance. The contours of position 4 showed some flattening on the upper and lower side of the contour due to the 3D-printed model. Lastly, the contour of position 5 was the hardest to obtain. This is because the kidney should be upright while making the contour figure. The kidney was balanced using the 3D-printed models, and the contour was twisted to some degrees. However, the quality of the 3D model was not decreased.

The 3D model of kidney 3 is of lower quality since the model has flattened edges due to the contour not completely fitting the FOV. However, this problem will be solved by adjusting the setup of the moorO_2Flo and extending the FOV.

Conducting the method and reaching the 3D model takes 10 minutes for each kidney. This duration is quick enough to produce the 3D models during the period of NMP. However, the method can be further improved and fastened by automatically selecting the contours from the color images of the kidney. Currently, this is performed manually, which is time-consuming. An improvement in the quality of the 3D model can be achieved by using more than three contours. However, the kidney must then be placed in more than three positions, which will take more time. Additionally, the current quality is sufficient to give a good picture of the overall appearance of the shape of the kidney.

3.4.2. Three-dimensional perfusion model

The method and setup developed to obtain a 3D visualization of the renal microcirculation resulted in a point cloud containing data from the surface perfusion. By using the six positions, perfusion data of the entire surface could be collected. The perfusion model is easy to read and provides quick insight into the perfusion distribution.

Experiments with induced ischemia validate the perfusion model's usefulness since the ischemia's location is clearly visible. In three out of four experiments, the ischemia caused by clamping the inferior branch of the artery resulted in evenly distributed ischemia over the inferior side of the kidney. However, in kidney 4, the ischemia was not evenly distributed. This was only noticeable by using the 3D perfusion model. The ischemia would not have been noticed if only the LSCI data of position 1 had been looked at to consider the kidney's quality. Therefore, visualizing the perfusion in 3D is necessary to obtain a correct view of the entire surface. For a future experiment, it would be interesting to cut open the kidney after NMP to indicate the vascular structure of the branches.

The perfusion model helps detect large areas with ischemia. However, whether the model can detect smaller areas with ischemia or areas with reduced perfusion has yet to be validated. An interesting improvement for the future would be to determine the sensitivity of the model. For example, it can be investigated which difference in blood flow is observable in the measured perfusion. It can also be investigated whether and how a longer warm ischemia time is visible in the perfusion model.

Determining the angle of incidence over the surface of the kidney has helped indicate perfusion data measured at an angle of incidence >40°. Perfusion data corresponding to data points with angles of incidence >40° is removed due to unreliability. In the model, these data points are indicated as white data points. In some cases, the determined angle of incidence of a data point was over or underestimated, resulting in the unnecessary removal or non-removal of data points. This can be improved by smoothening the angle of incidence model.

In the current model, data points correspond to angles of incidence from 0° to 40°. Since the measured perfusion decreases by 27% for 40°, still, not all data points are accurate. In addition, 40° is based on a small data set. To improve the process of compensating for the angle of incidence, it is valuable to do more research on the effect of the angle of incidence on the measured perfusion. Research should be done on the impact on the measured perfusion for more minor differences in the angle of incidence and at larger angles of incidence (angles >40°). If it is known what the consequences are per angle or incidence, the perfusion value can be adjusted for specific angles of incidence, reducing the removal of data points.

4

Conclusion

The goal of this thesis was to design a method to visualize the perfusion over the entire surface of normothermic machine-perfused kidneys using laser speckle contrast imaging. To reach this goal, the study was divided into smaller research objectives. First, the functioning of LSCI was investigated, and a method and setup were made to collect LSCI data from the convex kidney. The study outcomes indicate a strong positive linear correlation between the measured perfusion and the arterial blood flow for each kidney. From this, it could be concluded that the measured perfusion can be used to determine the quality of the perfusion of a single kidney over time.

By positioning the kidney in six different positions, it was possible to image the entire surface of the kidney. 3D models could be made from each kidney using the contours of three positions. The 3D models were used to give depth to the perfusion data of the corresponding positions. The perfusion over the entire surface of the kidney was visualized in a point cloud containing 3D coordinates of each position on the surface of the kidney and the corresponding perfusion value. Since the measured perfusion decreased significantly for increasing angles of incidence (a 27% decrease in perfusion for 40°), data collected at positions having an angle of incidence >40° was not used in the final 3D visualization.

Validating the perfusion model with induced ischemia caused by partly clamping the artery showed that the 3D visualization can indicate significant perfusion differences caused by ischemia. This makes LSCI a promising method for perfusion quality assessment. The method can be improved further by performing more research on the influence of the angle of incidence on the measured perfusion, both for more minor differences in the angle of incidence and for angles of incidence >40°.

A

LSCI protocol

Materials

- Porcine kidney
- NMP setup (including reservoir)
- moorO_2Flo device
- LSCI laptop Erasmus MC
- Black cloth
- 3D-printed model for positions 3 and 4
- 3D-printed model for positions 5 and 6
- Artery clamp
- Medical tweezers
- Protractor triangle

Method

Part 1 - Up to and including connecting kidney to NMP

1. Prepare the NMP setup according to the corresponding NMP protocol.
2. Prepare the kidney by removing fat and excessive tissue and connecting an arterial cannula.
3. Set camera settings moorO_2Flo
   (a) Camera control
      i. Zoom → kidney in FOV
      ii. Focus → automatic
      iii. Camera gain → automatic
      iv. LED brightness → automatic
   (b) Image settings
      i. Resolution → low
      ii. Low pass filter → 1.0 s

iii. Frame rate → 20 Hz (159 MB/min)

iv. Duration → 30 s

4. Darken the environment by placing black cloth over the moorO_2Flo device and NMP setup.
5. Place the kidney in position 1.
6. Start NMP by connecting the arterial cannula to the setup.

Part 2 - First 100 minutes of NMP

7. After 10 minutes of NMP take a LSCI recording. Make sure the kidney is in the FOV.
8. Read and write down the arterial flow (in mL/min) during the recording and the time (hh:mm) in Table A.1.
9. Save the LSCI recording.
10. Repeat steps 7, 8 and 9 after 20, 30, 40, 50, 60, 70, 80, 90 and 100 minutes of NMP.

Position of kidney	1	1	1	1	1	1	1	1	1	1
Duration of NMP (min)	10	20	30	40	50	60	70	80	90	100
Time (hh:mm)										
Flow (mL/min)										

Table A.1: Table to fill in time and flow during first 100 minutes of NMP.

Part 3 - LSCI recordings with the kidney in different positions before clamping

11. Take a LSCI recording of the kidney. Make sure the kidney is in the FOV.
12. Read and write down the arterial flow (in mL/min) during the recording and the time (hh:mm) in Table A.2.
13. Save the LSCI recording.
14. Position the kidney in position 2. Check whether the flow remains constant, if not reposition the tubing.
15. Repeat steps 11, 12 and 13.
16. Position the kidney in position 3 using the 3D-printed model for positions 3 and 4. Check whether the flow remains constant, if not reposition the tubing.
17. Repeat steps 11, 12 and 13.
18. Position the kidney in position 4 using the 3D-printed model for positions 3 and 4. Check whether the flow remains constant, if not reposition the tubing.
19. Repeat steps 11, 12 and 13.
20. Position the kidney in position 5 using the 3D-printed model for positions 5 and 6. Check whether the flow remains constant, if not reposition the tubing.
21. Repeat steps 11, 12 and 13.
22. Position the kidney in position 6 using the 3D-printed model for positions 5 and 6. Check whether the flow remains constant, if not reposition the tubing.
23. Repeat steps 11, 12 and 13.
24. Reposition the kidney in position 1.

Position of kidney	1	2	3	4	5	6
Time (hh:mm)						
Flow (mL/min)						

Table A.2: Table to fill in time and flow during LSCI measurements of kidney placed in different positions before clamping.

Part 4 - LSCI recordings using different angles of incidence

25. Take a LSCI recording of the kidney in position 1. Make sure the kidney is in the FOV.
26. Read and write down the arterial flow (in mL/min) during the recording and the time (hh:mm) in Table A.3.
27. Save the LSCI recording.
28. Adjust the angle of incidence using a protractor to 10° and repeat steps 25, 26 and 27.
29. Adjust the angle of incidence using a protractor to 20° and repeat steps 25, 26 and 27.
30. Adjust the angle of incidence using a protractor to 30° and repeat steps 25, 26 and 27.
31. Adjust the angle of incidence using a protractor to 40° and repeat steps 25, 26 and 27.
32. Adjust the angle of incidence using a protractor to 0°.

Position of kidney	1	1	1	1	1
Angle of incidence (deg)	0	10	20	30	40
Time (hh:mm)					
Flow (mL/min)					

Table A.3: Table to fill in time and flow during LSCI measurements with changing angle of incidence.

Part 5 - LSCI recordings with the kidney in different positions after clamping

33. Clamp the inferior branch of the renal artery with the artery clamp. Use medical tweezers to expose the artery.
34. Wait 15 minutes.
35. Take a LSCI recording of the kidney. Make sure the kidney is in the FOV.
36. Read and write down the arterial flow (in mL/min) during the recording and the time (hh:mm) in Table A.4.
37. Save the LSCI recording.
38. Position the kidney in position 2. Check whether the flow remains constant, if not reposition the tubing.
39. Repeat steps 35, 36 and 37.
40. Position the kidney in position 3 using the 3D-printed model for positions 3 and 4. Check whether the flow remains constant, if not reposition the tubing.
41. Repeat steps 35, 36 and 37.
42. Position the kidney in position 4 using the 3D-printed model for positions 3 and 4. Check whether the flow remains constant, if not reposition the tubing.
43. Repeat steps 35, 36 and 37.
44. Position the kidney in position 5 using the 3D-printed model for positions 5 and 6. Check whether the flow remains constant, if not reposition the tubing.

45. Repeat steps 35, 36 and 37.
46. Position the kidney in position 6 using the 3D-printed model for positions 5 and 6. Check whether the flow remains constant, if not reposition the tubing.
47. Repeat steps 35, 36 and 37.

Position of kidney	1	2	3	4	5	6
Time (hh:mm)						
Flow (mL/min)						

Table A.4: Table to fill in time and flow during LSCI measurements with kidney placed in different positions after clamping.

Part 6 - Ending NMP

48. Stop the NMP.
49. Remove the artery clamp.
50. Dispose the porcine blood and the kidney in the appropriate blue container.
51. Clean the setup.

B

Histograms of perfusion distribution in six different positions

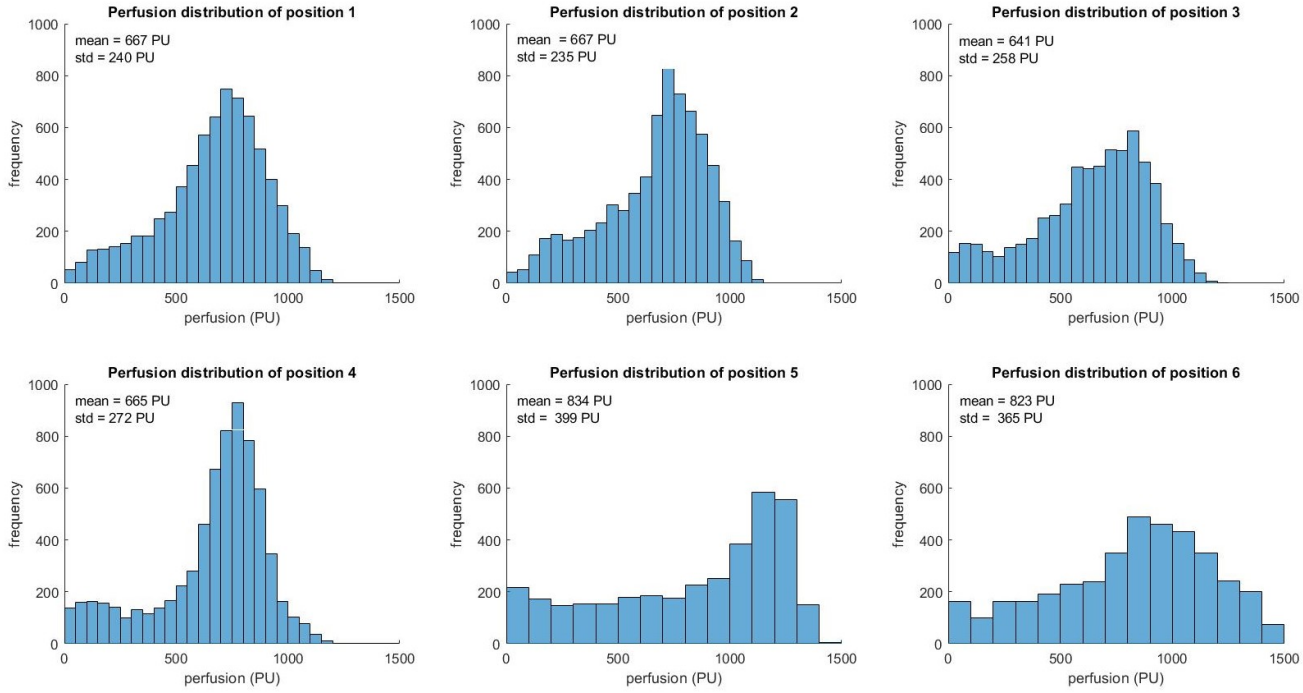

Figure B.1: Perfusion distribution per position for kidney 1 before clamping.

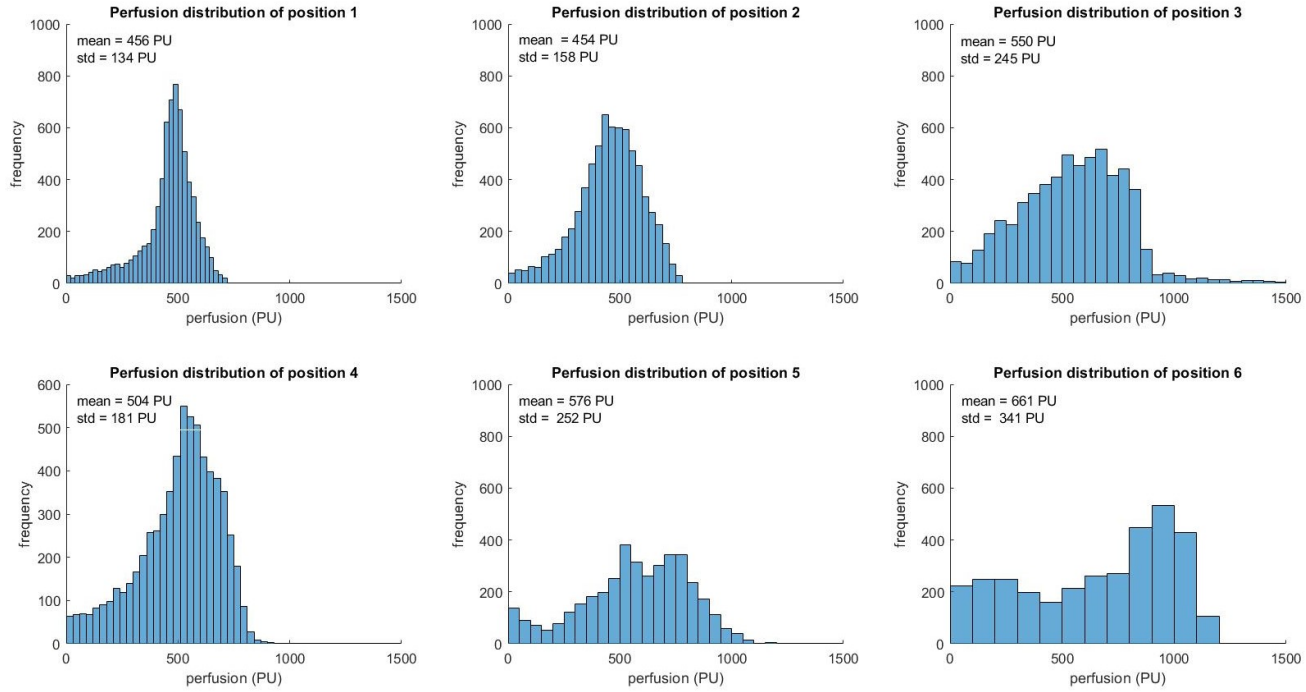

Figure B.2: Perfusion distribution per position for kidney 2 before clamping.

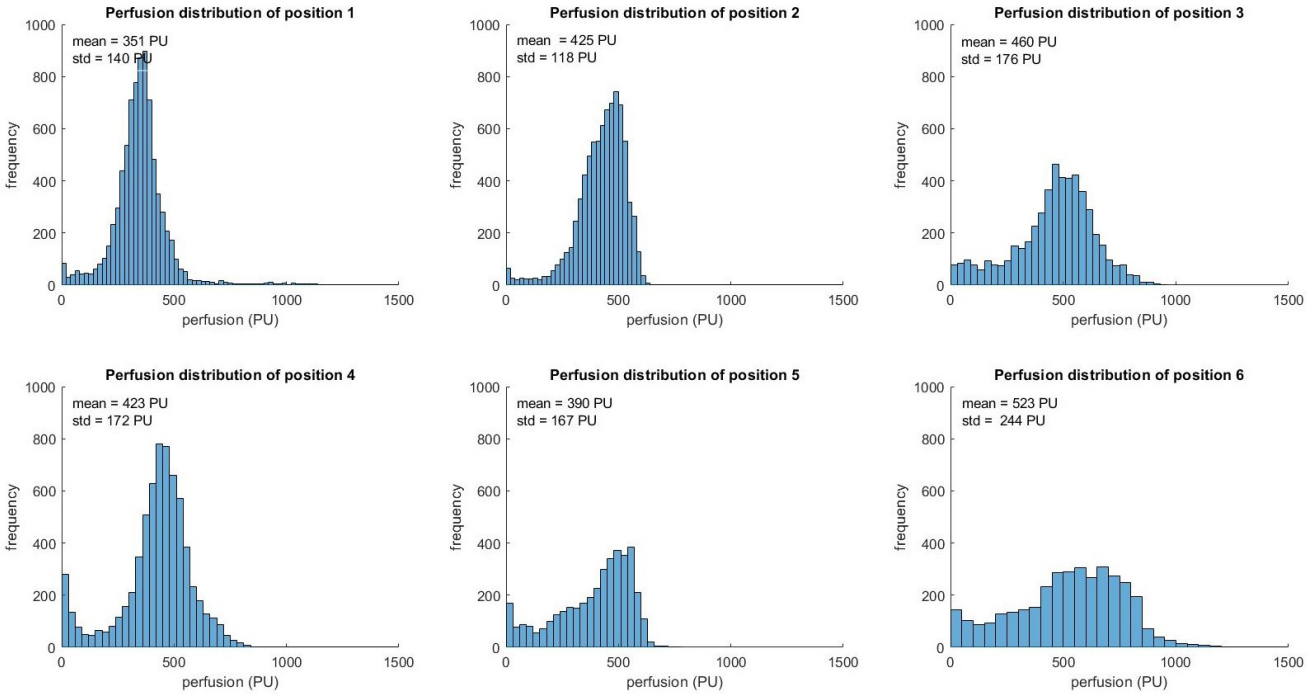

Figure B.3: Perfusion distribution per position for kidney 3 before clamping.

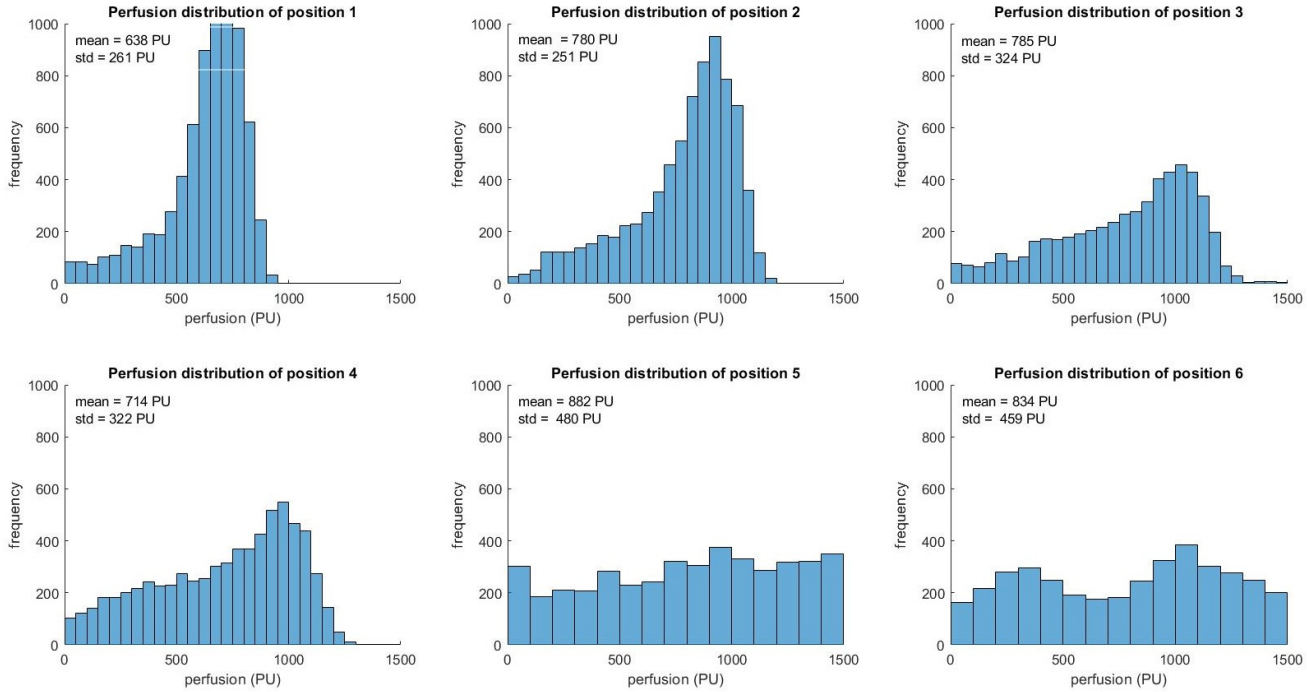

Figure B.4: Perfusion distribution per position for kidney 4 before clamping.

C

Photos of the kidney in six positions before and after clamping

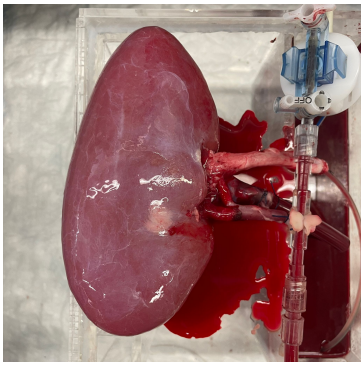

(a) Position 1 before clamping

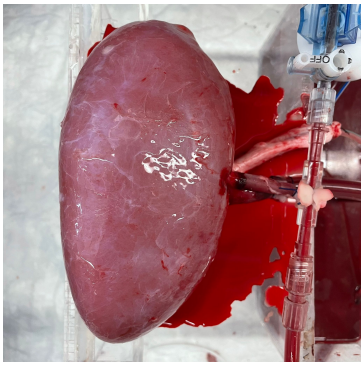

(b) Position 2 before clamping

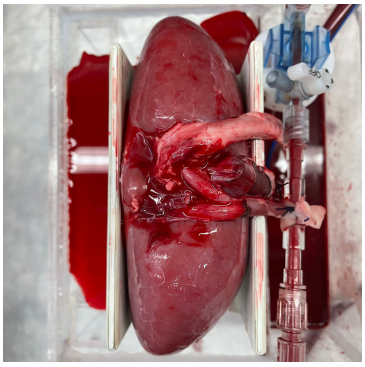

(c) Position 3 before clamping

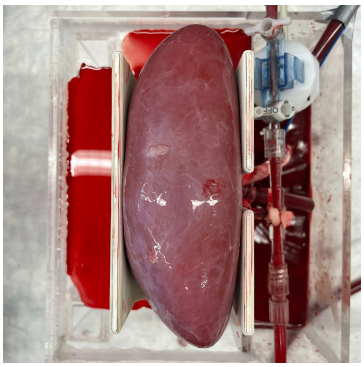

(d) Position 4 before clamping

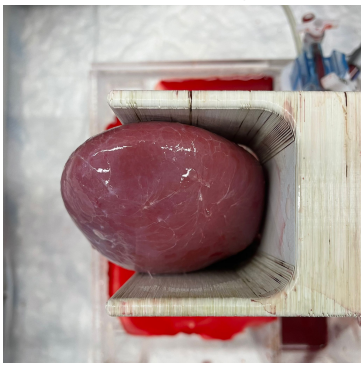

(e) Position 5 before clamping

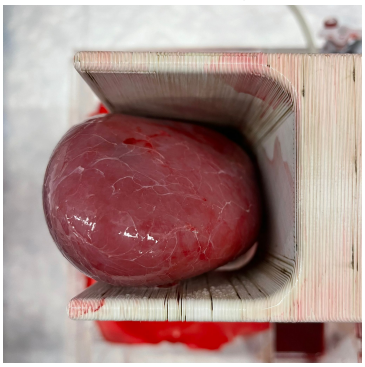

(f) Position 6 before clamping

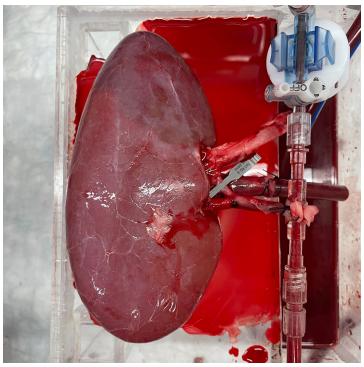

(g) Position 1 after clamping

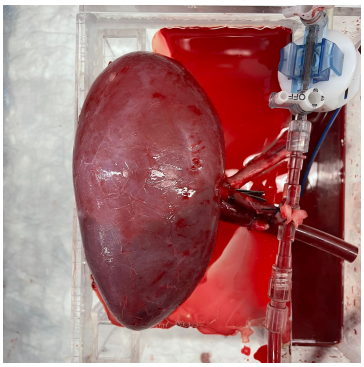

(h) Position 2 after clamping

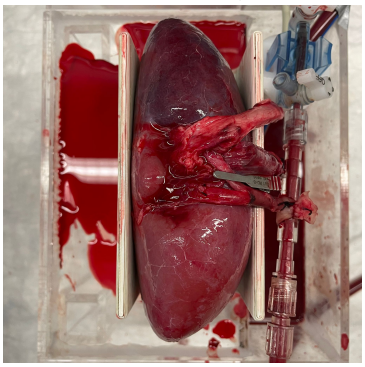

(i) Position 3 after clamping

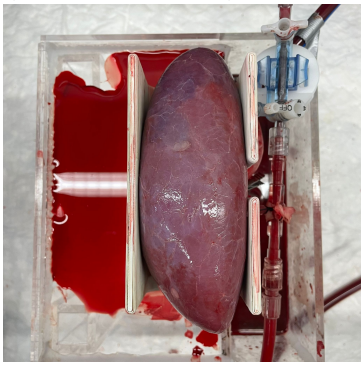

(j) Position 4 after clamping

(k) Position 5 after clamping

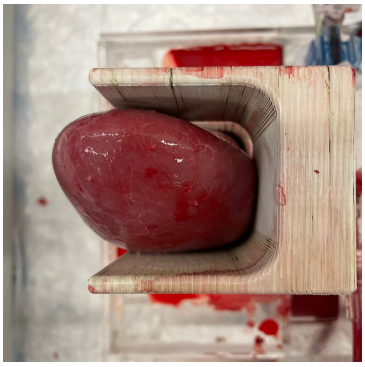

(l) Position 6 after clamping

Figure C.1: Color of a kidney during NMP before and after clamping the inferior branch of the artery in the different positions.

D

Matlab code 3D kidney model

```
clear all, close all, clc

%% Load contours
pos1 = imread('position1.png');
pos4 = imread('position4.png');
pos5 = imread('position5.png');

%% Crop figures
pos1( all(¬pos1,2), :) = []; % remove zero rows
pos1( :, all(¬pos1,1)) = []; % remove zero columns
pos4( all(¬pos4,2), :) = []; % remove zero rows
pos4( :, all(¬pos4,1)) = []; % remove zero columns
pos5( all(¬pos5,2), :) = []; % remove zero rows
pos5( :, all(¬pos5,1)) = []; % remove zero columns

%% Calculate ratios and resize images
Xpos4 = size(pos4, 1);
Xpos5 = size(pos5, 2);
Ypos1 = size(pos1, 2);
Ypos4 = size(pos4, 2);
Zpos1 = size(pos1, 1);
Zpos5 = size(pos5, 1);

xpixel = Xpos4;
ypixel = Ypos4;
zpixel = round((Xpos4 * Zpos5) / Xpos5);

pos1 = imresize(pos1, [zpixel ypixel]);
pos4 = imresize(pos4, [xpixel ypixel]);
pos5 = imresize(pos5, [zpixel xpixel]);

%% Create data 3D array
data_3D_square = zeros(xpixel,ypixel,zpixel);
% Basic model
for i = 1:xpixel
    for j = 1:ypixel
        for k = 1:zpixel
            if pos5(k,i) == 1 & pos4(i,j) == 1 & pos1(k,j) == 1
                data_3D_square(i,j,k) = 1;
            else
                data_3D_square(i,j,k) = 0;
            end
        end
    end
end

% Flip data to correct angle of view
data_3D_square = flip(data_3D_square, 1);
data_3D_square = flip(data_3D_square, 3);
```

```
50
51 volumeViewer(data_3D_square)
52
53 % Interpolated model
54 data_3D = data_3D_square;
55 for k = 1:zpixel
56     data_3D_slice = flip(squeeze(data_3D_square(:,:,k)),1);
57     [row,col] = find(data_3D_slice == 1);
58     difference_row = max(row)-min(row)+1;
59     difference_col = max(col)-min(col)+1;
60     pos4_small = imresize(pos4, [difference_row, difference_col]);
61     pos4_big = zeros(xpixel,ypixel);
62     pos4_big(min(row):max(row), min(col):max(col)) = pos4_small;
63     for r = 1:size(pos4_big,1)
64         for c = 1:size(pos4_big,2)
65             if pos4_big(r,c) < 0.2
66                 data_3D_slice(r,c) = 0;
67             end
68         end
69     end
70     data_3D(:, :, k)= flip(data_3D_slice, 2);
71 end
72
73 for j = 1:ypixel
74     data_3D_slice = flip(transpose(squeeze(data_3D_square(:,j,:))),1);
75     [row,col] = find(data_3D_slice == 1);
76     difference_row = max(row)-min(row)+1;
77     difference_col = max(col)-min(col)+1;
78     pos5_small = imresize(pos5, [difference_row, difference_col]);
79     pos5_big = zeros(zpixel,xpixel);
80     pos5_big(min(row):max(row), min(col):max(col)) = pos5_small;
81     for r = 1:size(pos5_big,1)
82         for c = 1:size(pos5_big,2)
83             if pos5_big(r,c) < 0.2
84                 data_3D_slice(r,c) = 0;
85             end
86         end
87     end
88     data_3D(:, j, :)= flip(transpose(data_3D_slice), 2);
89 end
90
91 for i = 1:xpixel
92     data_3D_slice = flip(transpose(squeeze(data_3D_square(i,:,:))),1);
93     [row,col] = find(data_3D_slice == 1);
94     difference_row = max(row)-min(row)+1;
95     difference_col = max(col)-min(col)+1;
96     pos1_small = imresize(pos1, [difference_row, difference_col]);
97     pos1_big = zeros(zpixel,ypixel);
98     pos1_big(min(row):max(row), min(col):max(col)) = pos1_small;
99     for r = 1:size(pos1_big,1)
100        for c = 1:size(pos1_big,2)
101            if pos1_big(r,c) == 0
102                data_3D_slice(r,c) = 0;
103            end
104        end
105    end
106    data_3D(i, :, :)= flip(transpose(data_3D_slice), 2);
107 end
108
109 % Smoothed model
110 data_3D = smooth3(data_3D);
111
112 %% Visualize model using volumeviewer
113 volumeViewer(data_3D)
```

E

Matlab code 3D perfusion model

```
%% %% Matlab code to make 3D perfusion model
clear all, close all, clc

%% Input
% 3D model
load('data_3D.mat');

% Size of 3D model
xpixel = size(data_3D,1);
ypixel = size(data_3D,2);
zpixel = size(data_3D,3);

% Perfusion data of each position
load('perfusion_pos1.mat');
load('perfusion_pos2.mat');
load('perfusion_pos3.mat');
load('perfusion_pos4.mat');
load('perfusion_pos5.mat');
load('perfusion_pos6.mat');

% Black and white contour figures (resize to 116 x 150 pixels)
contour1 = imresize(imread('Label_1.png'),[116 150]);
contour2 = imresize(imread('Label_2.png'),[116 150]);
contour3 = imresize(imread('Label_3.png'),[116 150]);
contour4 = imresize(imread('Label_4.png'),[116 150]);
contour5 = imresize(imread('Label_5.png'),[116 150]);
contour6 = imresize(imread('Label_6.png'),[116 150]);

% Variables read from MoorO2Flo files
length_y1  = 168.5     % Length of kidney in -ydirection (mm) in pos 1
distance_1 = 326.0     % Distance between laser and kidney (mm) in pos 1
length_y2  = 166.0     % Length of kidney in -ydirection (mm) in pos 2
distance_2 = 326.0     % Distance between laser and kidney (mm) in pos 2
length_x3  = 62.1      % Length of kidney in -xdirection (mm) in pos 3
distance_3 = 326.0     % Distance between laser and kidney (mm) in pos 3
length_x4  = 64.7      % Length of kidney in -xdirection (mm) in pos 4
distance_4 = 326.0     % Distance between laser and kidney (mm) in pos 4
length_z5  = 91.2      % Length of kidney in -zdirection (mm) in pos 5
distance_5 = 326.0     % Distance between laser and kidney (mm) in pos 5
length_z6  = 101.4     % Length of kidney in -zdirection (mm) in pos 6
distance_6 = 326.0     % Distance between laser and kidney (mm) in pos 6

%% Remove background from perfusion data
width  = 150;
height = 116;
for w = 1:width
    for h = 1:height
        if contour1(h,w) == 0;
            perfusion_pos1(h,w) = 0;
```

```
50          end
51          if contour2(h,w) == 0;
52              perfusion_pos2(h,w) = 0;
53          end
54          if contour3(h,w) == 0;
55              perfusion_pos3(h,w) = 0;
56          end
57          if contour4(h,w) == 0;
58              perfusion_pos4(h,w) = 0;
59          end
60          if contour5(h,w) == 0;
61              perfusion_pos5(h,w) = 0;
62          end
63          if contour6(h,w) == 0;
64              perfusion_pos6(h,w) = 0;
65          end
66      end
67  end
68
69  %% Crop perfusion images
70  % Remove zero rows
71  perfusion_pos1( all(¬perfusion_pos1,2), : ) = [];
72  perfusion_pos2( all(¬perfusion_pos2,2), : ) = [];
73  perfusion_pos3( all(¬perfusion_pos3,2), : ) = [];
74  perfusion_pos4( all(¬perfusion_pos4,2), : ) = [];
75  perfusion_pos5( all(¬perfusion_pos5,2), : ) = [];
76  perfusion_pos6( all(¬perfusion_pos6,2), : ) = [];
77  % Remove zero columns
78  perfusion_pos1( :, all(¬perfusion_pos1,1) ) = [];
79  perfusion_pos2( :, all(¬perfusion_pos2,1) ) = [];
80  perfusion_pos3( :, all(¬perfusion_pos3,1) ) = [];
81  perfusion_pos4( :, all(¬perfusion_pos4,1) ) = [];
82  perfusion_pos5( :, all(¬perfusion_pos5,1) ) = [];
83  perfusion_pos6( :, all(¬perfusion_pos6,1) ) = [];
84
85  %% Calculate depth of each position
86      % Position 1
87  perfusion_pos1 = imresize(perfusion_pos1, [zpixel ypixel]);
88  perfusion_pos1 = flip(perfusion_pos1,1);
89  depth_pos1 = zeros(zpixel, ypixel);
90  for k = 1:zpixel
91      for j = 1:ypixel
92          for i = 1:xpixel
93              if data_3D(i,j,k) > 0
94                  depth_pos1(k,j) = i;
95                  break
96              else
97                  depth_pos1(k,j) = NaN;
98              end
99          end
100     end
101 end
102
103     % Position 2
104 perfusion_pos2 = imresize(perfusion_pos2, [zpixel ypixel]);
105 perfusion_pos2 = flip(perfusion_pos2,1);
106 depth_pos2 = zeros(zpixel, ypixel);
107 for k = 1:zpixel
108     for j = 1:ypixel
109         for i = 1:xpixel
110             if data_3D(xpixel-i+1,j,k) > 0
111                 depth_pos2(k,j) = xpixel-i+1;
112                 break
113             else
114                 depth_pos2(k,j) = NaN;
115             end
116         end
117     end
118 end
119
120     % Position 3
```

```
perfusion_pos3 = imresize(perfusion_pos3, [xpixel ypixel]);
depth_pos3 = zeros(xpixel, ypixel);
for i = 1:xpixel
    for j = 1:ypixel
        for k = 1:zpixel
            if data_3D(i,j,k) > 0
                depth_pos3(i,j) = k;
                break
            else
                depth_pos3(i,j) = NaN;
            end
        end
    end
end

    % Position 4
perfusion_pos4 = imresize(perfusion_pos4, [xpixel ypixel]);
depth_pos4 = zeros(xpixel, ypixel);
for i = 1:xpixel
    for j = 1:ypixel
        for k = 1:zpixel
            if data_3D(i,j,(zpixel-k+1)) > 0
                depth_pos4(i,j) = (zpixel-k+1);
                break
            else
                depth_pos4(i,j) = NaN;
            end
        end
    end
end

    % Position 5
perfusion_pos5 = imresize(perfusion_pos5, [zpixel xpixel]);
perfusion_pos5 = flip(perfusion_pos5,1);
perfusion_pos5 = flip(perfusion_pos5,2);
depth_pos5 = zeros(zpixel, xpixel);
for k = 1:zpixel
    for i = 1:xpixel
        for j = 1:ypixel
            if data_3D(i,j,k) > 0
                depth_pos5(k,i) = ypixel-j+1;
                break
            else
                depth_pos5(k,i) = NaN;
            end
        end
    end
end

    % Position 6
perfusion_pos6 = imresize(perfusion_pos6, [zpixel xpixel]);
depth_pos6 = zeros(zpixel, xpixel);
for k = 1:zpixel
    for i = 1:xpixel
        for j = 1:ypixel
            if data_3D(i, (ypixel-j+1),k) > 0
                depth_pos6(k,i) = j;
                break
            else
                depth_pos6(k,i) = NaN;
            end
        end
    end
end

%% Calculate angle of incidence of each position
    % Position 1
% Normal vector for each data point and reverse direction
 [Nx,Ny,Nz] =surfnorm(depth_pos1);
Nx = -1*Nx;
Ny = -1*Ny;
```

```
192 Nz = -1*Nz;
193 N = reshape([Nx Ny Nz], zpixel,ypixel,3);
194
195 % Vector of laser incidence on each data point
196 distancepixel_1 = round(distance_1* ypixel / length_y1); % distance in pixels from ...
        kidney to laser
197 x = round(size(depth_pos1,1)/2);
198 y = round(size(depth_pos1,2)/2);
199 z = -1*distancepixel_1;
200 pos_laser_1 = [x;y;z];
201
202 % Define angle of incidence of each point using equation 3.1
203 angle_pos1 = zeros(zpixel,ypixel);
204 for j = 1:ypixel
205     for k = 1:zpixel
206         vector_kidney = squeeze(N(k,j,:));
207         vector_lasertokidney = [depth_pos1(k,j);j;k] - pos_laser_1;
208         A_dot_B = dot(vector_lasertokidney,vector_kidney);
209         A = norm(vector_lasertokidney);
210         B = norm(vector_kidney);
211         angle_pos1(k,j) = 180 - acosd( A_dot_B / (A*B) );
212     end
213 end
214
215 % Flip arrays
216 depth_pos1 = flip(depth_pos1,2);
217 perfusion_pos1 = flip(perfusion_pos1,2);
218 angle_pos1 = flip(angle_pos1,2);
219
220     % Position 2
221 perfusion_pos2 = flip(perfusion_pos2,2);
222 % Normal vector for each data point and reverse direction
223 [Nx,Ny,Nz] =surfnorm(depth_pos2);
224 Nx = -1*Nx;
225 Ny = -1*Ny;
226 Nz = -1*Nz;
227 N = reshape([Nx Ny Nz], zpixel,ypixel,3);
228
229 % Vector of laser incidence on each data point
230 distancepixel_2 = round(distance_2* ypixel / length_y2); % distance in pixels from ...
        kidney to laser
231 x = round(size(depth_pos2,1)/2);
232 y = round(size(depth_pos2,2)/2);
233 z = -1*distancepixel_2;
234 pos_laser_2 = [x;y;z];
235
236 % Define angle of incidence of each point using equation 3.1
237 angle_pos2 = zeros(zpixel,ypixel);
238 for j = 1:ypixel
239     for k = 1:zpixel
240         vector_kidney = squeeze(N(k,j,:));
241         vector_lasertokidney = [depth_pos2(k,j);j;k] - pos_laser_2;
242         A_dot_B = dot(vector_lasertokidney,vector_kidney);
243         A = norm(vector_lasertokidney);
244         B = norm(vector_kidney);
245         angle_pos2(k,j) = 180 - acosd( A_dot_B / (A*B) );
246     end
247 end
248
249 % Flip arrays
250 angle_pos2 = flip(angle_pos2,2);
251 depth_pos2 = flip(depth_pos2,2);
252 perfusion_pos2 = flip(perfusion_pos2,2);
253
254     % Position 3
255 % Normal vector for each data point and reverse direction
256 [Nx,Ny,Nz] =surfnorm(depth_pos3);
257 Nx = -1*Nx;
258 Ny = -1*Ny;
259 Nz = -1*Nz;
260 N = reshape([Nx Ny Nz], xpixel,ypixel,3);
```

```
261
262 % Vector of laser incidence on each data point
263 distancepixel_3 = round(distance_3* xpixel / length_x3); % distance in pixels from ...
        kidney to laser
264 x = round(size(depth_pos3,1)/2);
265 y = round(size(depth_pos3,2)/2);
266 z = -1*distancepixel_3;
267 pos_laser_3 = [x;y;z];
268
269 % Define angle of incidence of each point using equation 3.1
270 angle_pos3 = zeros(xpixel,ypixel);
271 for i = 1:xpixel
272     for j = 1:ypixel
273         vector_kidney = squeeze(N(i,j,:));
274         vector_lasertokidney = [i; j; depth_pos3(i,j)] - pos_laser_3;
275         A_dot_B = dot(vector_lasertokidney,vector_kidney);
276         A = norm(vector_lasertokidney);
277         B = norm(vector_kidney);
278         angle_pos3(i,j) = 180 - acosd( A_dot_B / (A*B) );
279     end
280 end
281
282 % Flip arrays
283 depth_pos3 = flip(depth_pos3,2);
284 perfusion_pos3 = flip(perfusion_pos3,2);
285 angle_pos3 = flip(angle_pos3,2);
286
287     % Position 4
288 depth_pos4 = flip(depth_pos4,1);
289 % Normal vector for each data point and reverse direction
290 [Nx,Ny,Nz] =surfnorm(depth_pos4);
291 Nx = -1*Nx;
292 Ny = -1*Ny;
293 Nz = -1*Nz;
294 N = reshape([Nx Ny Nz], xpixel,ypixel,3);
295
296 % Vector of laser incidence on each data point
297 distancepixel_4 = round(distance_4* xpixel / length_x4); % distance in pixels from ...
        kidney to laser
298 x = round(size(depth_pos4,1)/2);
299 y = round(size(depth_pos4,2)/2);
300 z = -1*distancepixel_4;
301 pos_laser_4 = [x;y;z];
302
303 % Define angle of incidence of each point using equation 3.1
304 angle_pos4 = zeros(xpixel,ypixel);
305 for i = 1:xpixel
306     for j = 1:ypixel
307         vector_kidney = squeeze(N(i,j,:));
308         vector_lasertokidney = [i; j; depth_pos4(i,j)] - pos_laser_4;
309         A_dot_B = dot(vector_lasertokidney,vector_kidney);
310         A = norm(vector_lasertokidney);
311         B = norm(vector_kidney);
312         angle_pos4(i,j) = 180 - acosd( A_dot_B / (A*B) );
313     end
314 end
315
316 % Flip arrays
317 depth_pos4 = flip(depth_pos4,1);
318 depth_pos4 = flip(depth_pos4,2);
319 perfusion_pos4 = flip(perfusion_pos4,1);
320 perfusion_pos4 = flip(perfusion_pos4,2);
321 angle_pos4 = flip(angle_pos4,1);
322 angle_pos4 = flip(angle_pos4,2);
323
324     % Position 5
325 perfusion_pos5 = flip(perfusion_pos5,2);
326 depth_pos5 = flip(depth_pos5,2);
327 % Normal vector for each data point and reverse direction
328 [Nx,Ny,Nz] =surfnorm(depth_pos5);
329 Nx = -1*Nx;
```

```
330 Ny = -1*Ny;
331 Nz = -1*Nz;
332 N = reshape([Nx Ny Nz], zpixel,xpixel,3);
333
334 % Vector of laser incidence on each data point
335 distancepixel_5 = round(distance_5* zpixel / length_z5); % distance in pixels from ...
        kidney to laser
336 x = round(size(depth_pos5,1)/2);
337 y = round(size(depth_pos5,2)/2);
338 z = -1*distancepixel_5;
339 pos_laser_5 = [x;y;z];
340
341 % Define angle of incidence of each point using equation 3.1
342 angle_pos5 = zeros(zpixel,xpixel);
343 for k = 1:zpixel
344     for i = 1:xpixel
345         vector_kidney = squeeze(N(k,i,:));
346         vector_lasertokidney = [i; depth_pos5(k,i); k] - pos_laser_5;
347         A_dot_B = dot(vector_lasertokidney,vector_kidney);
348         A = norm(vector_lasertokidney);
349         B = norm(vector_kidney);
350         angle_pos5(k,i) = 180 - acosd( A_dot_B / (A*B) );
351     end
352 end
353
354 % Flip arrays
355 perfusion_pos5 = flip(perfusion_pos5,2);
356 depth_pos5 = flip(depth_pos5,2);
357 angle_pos5 = flip(angle_pos5,2);
358
359     % Position 6
360 % Normal vector for each data point and reverse direction
361 [Nx,Ny,Nz] =surfnorm(depth_pos6);
362 Nx = -1*Nx;
363 Ny = -1*Ny;
364 Nz = -1*Nz;
365 N = reshape([Nx Ny Nz], zpixel,xpixel,3);
366
367 % Vector of laser incidence on each data point
368 distancepixel_6 = round(distance_6* zpixel / length_z6); % distance in pixels from ...
        kidney to laser
369 x = round(size(depth_pos6,1)/2);
370 y = round(size(depth_pos6,2)/2);
371 z = -1*distancepixel_6;
372 pos_laser_6 = [x;y;z];
373
374 % Define angle of incidence of each point using equation 3.1
375 angle_pos6 = zeros(zpixel,xpixel);
376 for k = 1:zpixel
377     for i = 1:xpixel
378         vector_kidney = squeeze(N(k,i,:));
379         vector_lasertokidney = [i; depth_pos6(k,i);k] - pos_laser_6;
380         A_dot_B = dot(vector_lasertokidney,vector_kidney);
381         A = norm(vector_lasertokidney);
382         B = norm(vector_kidney);
383         angle_pos6(k,i) = 180 - acosd( A_dot_B / (A*B) );
384     end
385 end
386
387 % Flip arrays
388 perfusion_pos6 = flip(perfusion_pos6,1);
389
390 %% Create point cloud
391 count1 = 1;
392 count2 = 1;
393 count3 = 1;
394 count4 = 1;
395 count5 = 1;
396 count6 = 1;
397
398 % Store data of 3D coordinates (x,y,z) and corresponding perfusion color
```

```
% Assign color 0 if angle of incidence > 40 degrees
% Assign color corresponding to perfusion value if angle ≤ 40 degrees

    % Position 1
for j = 1:ypixel
    for k = 1:zpixel
            if (depth_pos1(k,j) > 0) && (angle_pos1(k,j) ≤ 40)
                color1 = round(perfusion_pos1(k,j)/1000*256);
                datapos1(count1,:) = [depth_pos1(k,j), j, k, color1, 1];
                count1 = count1 + 1;
            elseif (depth_pos1(k,j) > 0 ) && (angle_pos1(k,j) > 40)
                datapos1(count1,:) = [depth_pos1(k,j), j, k, 0, 1];
                count1 = count1 + 1;
            end
    end
end
    % Position 2
for j = 1:ypixel
    for k = 1:zpixel
        if (depth_pos2(k,j) > 0) && (angle_pos2(k,j) ≤ 40)
            color2 = round(perfusion_pos2(k,j)/1000*256);
            datapos2(count2,:) = [depth_pos2(k,j), j, k, color2, 2];
            count2 = count2 + 1;
        elseif (depth_pos2(k,j) > 0) && (angle_pos2(k,j) > 40)
            datapos2(count2,:) = [depth_pos2(k,j), j, k, 0, 2];
            count2 = count2 + 1;
        end
    end
end
    % Position 3
for i = 1:xpixel
    for j = 1:ypixel
            if (depth_pos3(i,j) > 0) && (angle_pos3(i,j) ≤ 40)
                color3 = round(perfusion_pos3(i,j)/1000*256);
                datapos3(count3,:) = [i, j, depth_pos3(i,j), color3, 3];
                count3 = count3 + 1;
            elseif (depth_pos3(i,j) > 0 ) && (angle_pos3(i,j) > 40)
                datapos3(count3,:) = [i, j, depth_pos3(i,j), 0, 3];
                count3 = count3 + 1;
            end
    end
end
    % Position 4
for i = 1:xpixel
    for j = 1:ypixel
        if (depth_pos4(i,j) > 0) && (angle_pos4(i,j) ≤ 40)
            color4 = round(perfusion_pos4(i,j)/1000*256);
            datapos4(count4,:) = [i, j, depth_pos4(i,j), color4, 4];
            count4 = count4 + 1;
        elseif (depth_pos4(i,j) > 0 ) && (angle_pos4(i,j) > 40)
            datapos4(count4,:) = [i, j, depth_pos4(i,j), 0, 4];
            count4 = count4 + 1;
        end
    end
end
    % Position 5
for i = 1:xpixel
    for k = 1:zpixel
        if (depth_pos5(k,i) > 0 ) && (angle_pos5(k,i) ≤ 40)
            color5 = round(perfusion_pos5(k,i)/1000*256);
            datapos5(count5,:) = [i, depth_pos5(k,i), k, color5, 5];
            count5 = count5 + 1;
        elseif (depth_pos5(k,i) > 0 ) && (angle_pos5(k,i) > 40)
            datapos5(count5,:) = [i, depth_pos5(k,i), k, 0, 5];
            count5 = count5 + 1;
        end
    end
end
    % Position 6
for i = 1:xpixel
    for k = 1:zpixel
```

```
470         if (depth_pos6(k,i) > 0 ) && (angle_pos6(k,i) ≤ 40)
471             color6 = round(perfusion_pos6(k,i)/1000*256);
472             datapos6(count6,:) = [i, depth_pos6(k,i), k, color6, 6];
473             count6 = count6 + 1;
474         elseif (depth_pos6(k,i) > 0 ) && (angle_pos6(k,i) > 40)
475             datapos6(count6,:) = [i, depth_pos6(k,i), k, 0, 6];
476             count6 = count6 + 1;
477         end
478     end
479 end
480
481 % Merge data
482 datapos12 = union(datapos1, datapos2, 'rows');
483 datapos123 = union(datapos12, datapos3, 'rows');
484 datapos1234 = union(datapos123, datapos4, 'rows');
485 datapos12345 = union(datapos1234, datapos5, 'rows');
486 datapos = union(datapos12345, datapos6, 'rows');
487
488 % Sort data (on coordinate and on perfusion value)
489 datapossort = sortrows(datapos, [1 2 3 4]);
490
491 % Remove non-unique coordinates (keep highest perfusion value coordinate)
492 [¬,uniquepoints] = unique(datapossort(:,(1:3)),'rows', 'last');
493 dataposnew = datapossort(uniquepoints,:);
494
495 % Make point cloud
496 count = 1;
497 c = jet;
498 for i = 1 : size(dataposnew,1)
499     if dataposnew(i,4) > 256
500         colorpointcloud(count,1) = c(256,1);    % Assign RGB color (1/3)
501         colorpointcloud(count,2) = c(256,2);    % Assign RGB color (2/3)
502         colorpointcloud(count,3) = c(256,3);    % Assign RGB color (3/3)
503         pointcloud(count,:) = dataposnew(i, (1:3));   % Assign 3D coordinate
504         count = count + 1;
505     elseif dataposnew(i,4) < 1
506         colorpointcloud(count,1) = 255;         % Assign RGB color white (1/3)
507         colorpointcloud(count,2) = 255;         % Assign RGB color white (2/3)
508         colorpointcloud(count,3) = 255;         % Assign RGB color white (3/3)
509         pointcloud(count,:) = dataposnew(i, (1:3));   % Assign 3D coordinate
510         count = count + 1;
511     else
512         colorpointcloud(count,1) = c(dataposnew(i,4),1); % Assign RGB color (1/3)
513         colorpointcloud(count,2) = c(dataposnew(i,4),2); % Assign RGB color (2/3)
514         colorpointcloud(count,3) = c(dataposnew(i,4),3); % Assign RGB color (3/3)
515         pointcloud(count,:) = dataposnew(i, (1:3));   % Assign 3D coordinate
516         count = count + 1;
517     end
518 end
519
520 ptCloud = pointCloud(pointcloud, 'Color', colorpointcloud)
521 pcwrite(ptCloud, 'pointcloudnierXX.ply')    % Save point cloud
```

Bibliography

[1] C.B. Abela and S. Homer-Vanniasinkham. “Clinical implications of ischaemia-reperfusion injury”. In: *Pathophysiology: the official journal of the International Society for Pathophysiology* 9.4 (2003), pp. 229–240. DOI: https://doi.org/10.1016/s0928-4680(03)00025-7.

[2] D.A. Boas and A.K. Dunn. “Laser speckle contrast imaging in biomedical optics”. In: *Journal of Biomedical Optics* 15.1 (2010). 011109. DOI: https://doi.org/10.1117/1.3285504.

[3] J.D. Briers and S. Webster. “Laser speckle contrast analysis (LASCA): a nonscanning, full-field technique for monitoring capillary blood flow”. In: *Journal of Biomedical Optics* 1.2 (1996), pp. 174–179. DOI: https://doi.org/10.1117/12.231359.

[4] J.D. Briers et al. “Laser speckle contrast imaging: theoretical and practical limitations”. In: *Journal of Biomedical Optics* 18.6 (2013). 066018. DOI: https://doi.org/10.1117/1.JBO.18.6.066018.

[5] T.M. Buzug. “Computed Tomography”. In: *Springer Handbook of Medical Technology*. Berlin, Heidelberg: Springer, 2011, pp. 311–342.

[6] Y. Chen et al. “Preservation Solutions for Kidney Transplantation: History, Advances and Mechanisms”. In: *Cell Transplantation* 28.12 (2019), pp. 1472–1489. DOI: https://doi.org/10.1177/0963689719872699.

[7] D.B. Conkey, A.M. Caravaca-Aguirre, and R. Piestun. “High-speed scattering medium characterization with application to focusing light through turbid media”. In: *Optics Express* 20.2 (2012), pp. 1733–1740. DOI: https://doi.org/10.1364/OE.20.001733.

[8] M.A. Davis, S.M. Shams Kazmi, and A.K. Dunn. “Imaging depth and multiple scattering in laser speckle contrast imaging”. In: *Journal of Biomedical Optics* 19.8 (2014). 086001. DOI: https://doi.org/10.1117/1.JBO.19.8.086001.

[9] B. Dorweiler et al. “Ischemia-Reperfusion Injury: Pathophysiology and Clinical Implications”. In: *European journal of trauma and emergency surgery* 33.6 (2007), pp. 600–612. DOI: https://doi.org/10.1007/s00068-007-7152-z.

[10] A.K. Dunn et al. “Dynamic Imaging of Cerebral Blood Flow Using Laser Speckle”. In: *Journal of Cerebral Blood Flow and Metabolism* 21.3 (2001), pp. 195–201. DOI: https://doi.org/10.1097/00004647-200103000-00002.

[11] A.F. Fercher and J.D. Briers. “Flow visualization by means of single-exposure speckle photography”. In: *Optics Communications* 37.5 (1981), pp. 326–330. DOI: https://doi.org/10.1016/0030-4018(81)90428-4.

[12] K.R. Forrester et al. “A Laser Speckle Imaging Technique for Measuring Tissue Perfusion”. In: *IEEE transactions on bio-medical engineering* 51.11 (2004), pp. 2074–2084. DOI: https://doi.org/10.1109/TBME.2004.834259.

[13] B.J. Fuller and C.Y. Lee. “Hypothermic perfusion preservation: The future of organ preservation revisited?” In: *Cryobiology* 54.2 (2007), pp. 129–145. DOI: https://doi.org/10.1016/j.cryobiol.2007.01.003.

[14] S.B. Gokturk, H. Yalcin, and C. Bamji. “A Time-Of-Flight Depth Sensor - System Description, Issues and Solutions”. In: *Conference on Computer Vision and Pattern Recognition Workshop* (2004). 35. DOI: https://doi.org/10.1109/CVPR.2004.291.

[15] T.L. Hamelink et al. “Renal Normothermic Machine Perfusion: The Road Toward Clinical Implementation of a Promising Pretransplant Organ Assessment Tool”. In: *Transplantation* 106.2 (2022), pp. 268–279. DOI: https://doi.org/10.1097/TP.0000000000003817.

[16] W. Heeman et al. “Clinical applications of laser speckle contrast imaging: a review”. In: *Journal of Biomedical Optics* 24.8 (2019). 080901, pp. 1–11. DOI: https://doi.org/10.1117/1.JBO.24.8.080901.

[17] S.A. Hosgood, E. van Heurn, and M.L. Nicholson. “Normothermic machine perfusion of the kidney:better conditioning and repair?” In: *Transplant International* 28.6 (2015), pp. 657–664. DOI: https://doi.org/10.1111/tri.12319.

[18] S.A. Hosgood et al. “Ex vivo normothermic perfusion for quality assessment of marginal donor kidney transplants”. In: *The British journal of surgery* 102.11 (2015), pp. 1433–1440. DOI: https://doi.org/10.1002/bjs.9894.

[19] I. Jochmans et al. “Past, Present, and Future of Dynamic Kidney andLiver Preservation and Resuscitation”. In: *American Journal of Transplantation* 16.9 (2016), pp. 2545–2555. DOI: https://doi.org/10.1111/ajt.13778.

[20] F. Lindahl, E. Tesselaar, and F. Sjörberg. “Assessing paediatric scald injuries using Laser Speckle Contrast Imaging”. In: *Burns* 39.4 (2013), pp. 662–666. DOI: https://doi.org/10.1016/j.burns.2012.09.018.

[21] M. Lomero et al. “Donation after circulatory death today: an updated overview of the European landscape”. In: *Transplant International* 33.1 (2019), pp. 76–88. DOI: https://doi.org/10.1111/tri.13506.

[22] Moor Instruments Ltd. *moorO2Flo Perfusion and Oxygenation Imager Hardware User Manual*. English. Version 1. Moor Instruments Ltd. June 5, 2019. 17 pp.

[23] G. Mahé et al. “Distance between laser head and skin does not influence skin blood flow values recorded by laser speckle imaging”. In: *Microvascular research* 82.3 (2011), pp. 439–442. DOI: https://doi.org/10.1016/j.mvr.2011.06.014.

[24] E. N. Marieb and K. Hoehn. *Human Anatomy Physiology*. Pearson Education, 2016. ISBN: 1-292-09697-7.

[25] E. Molnár et al. “Assessment of the test-retest reliability of human gingival blood flow measurements by Laser Speckle Contrast Imaging in a healthy cohort”. In: *Microcirculation* 25.2 (2018). e12420. DOI: https://doi.org/10.1111/micc.12420.

[26] A.Y. Mülayim, U. Yilmaz, and V. Atalay. “Silhouette-Based 3-D Model Reconstruction From Multiple Images”. In: *IEEE Transactions on Systems, Man, and Cybernetics, Part B (Cybernetics)* 33.4 (2003), pp. 582–591. DOI: https://doi.org/10.1109/TSMCB.2003.814303.

[27] Nierstichting. *Feiten en cijfers*. URL: https://nierstichting.nl/over-nieren/hoe-werken-je-nieren/feiten-en-cijfers/ (visited on 04/06/2022).

[28] Nierstichting. *Feiten en cijfers*. URL: https://nierstichting.nl/leven-met-een-nierziekte/feiten-en-cijfers/ (visited on 04/07/2022).

[29] J.M. O’Callaghan et al. “Preservation Solutions for Static Cold Storage of Kidney Allografts: A Systematic Review and Meta-Analysis”. In: *American Journal of Transplantation* 12.4 (2012), pp. 896–906. DOI: https://doi.org/10.1111/j.1600-6143.2011.03908.x.

[30] C. Ponticelli. “Ischaemia-reperfusion injury: a major protagonist in kidney transplantation”. In: *Nephrology, dialysis, transplantation* 29.6 (2014), pp. 1134–1140. DOI: https://doi.org/10.1093/ndt/gft488.

[31] A. Ponticorvo and A.K. Dunn. “How to Build a Laser Speckle Contrast Imaging (LSCI) System to Monitor Blood Flow”. In: *Journal of visualized experiments* 45 (2010). DOI: https://doi.org/10.3791/2004.

[32] C.P. Price and H. Finney. “Developments in the assessment of glomerular filtration rate”. In: *Clinica Chimica Acta* 297.1-2 (2000), pp. 55–66. DOI: https://doi.org/10.1016/s0009-8981(00)00233-3.

[33] L.M. Richards et al. “Intraoperative multi-exposure speckle imaging of cerebral blood flow”. In: *Journal of Cerebral Blood Flow Metabolism* 37.9 (2017), pp. 3097–3109. DOI: https://doi.org/10.1177/0271678X16686987.

[34] J. Senarathna et al. “Laser Speckle Contrast Imaging: Theory, Instrumentation and Applications”. In: *IEEE reviews in biomedical engineering* 6 (2013), pp. 99–110. DOI: https://doi.org/10.1109/RBME.2013.2243140.

[35] C. Stoianovici, P. Wilders-Smith, and B. Choi. “Assessment of Pulpal Vitality Using Laser Speckle Imaging”. In: *Lasers in Surgery and Medicine* 43.8 (2011), pp. 833–837. DOI: https://doi.org/10.1002/lsm.21090.

[36] M. Timsit and S.G. Tullius. “Hypothermic kidney preservation: a remembrance of the past in the future?” In: *Current Opinion in Organ Transplantation* 16.2 (2011), pp. 162–168. DOI: https://doi.org/10.1097/MOT.0b013e3283446b07.

[37] P. Urbanellis et al. “Normothermic Ex Vivo Kidney Perfusion Improves Early DCD Graft Function Compared With Hypothermic Machine Perfusion and Static Cold Storage”. In: *Transplantation* 104.5 (2020), pp. 947–955. DOI: https://doi.org/10.1097/TP.0000000000003066.

[38] P. Vaz et al. “Laser Speckle Imaging to Monitor Microvascular Blood Flow: A Review”. In: *IEEE reviews in biomedical engineering* 9 (2016), pp. 106–120. DOI: https://doi.org/10.1109/RBME.2016.2532598.

[39] J. Zötterman et al. “Methodological concerns with laser speckle contrast imaging in clinical evaluation of microcirculation”. In: *PloS one* 12.3 (2017). e0174703. DOI: https://doi.org/10.1371/journal.pone.0174703.